Note to reader

This draft version of Chapter 3 in the Technical Background Report to the Global Mercury Assessment 2018 is made available for review by national representatives and experts. The draft version contains material that will be further refined and elaborated after the review process. Specific items where the content of this draft chapter will be further improved and modified are:

1. New data and trend analysis on Canadian monitoring data will be added
2. Maps and tables for data from USA will be revised and improved.
3. Additional information and evaluation of polar measurements will be added.
4. The map of ALL monitoring sites from all existing networks in section 2 will be further improved
5. References list will be further improved as soon as the revised final draft will be ready
6. Conclusions and main messages will be formulated.

GMA 2018 Draft Chapter 3. Levels of mercury in air. Nicola Pirrone, Mariantonia Bencardino, Sergio Cinnirella, Aurélien Dommergue, Joseph Timothy Dvonch, Ralf Ebinghaus, Xinbin Feng, Alessandra Fino, Xuewu Fu, Katarina Gårdfeldt, Antonella Macagnano, David Schmeltz, David Gay, Milena Horvat, Dan Jaffe, Joze Kotnic, Henrik Skov, Francesca Sprovieri, Helen Angot, Alexandra Steffen, Amanda Cole, Elsie Sunderland, Kjetil Torseth, Simon Wilson (Members of the UNEP Fate & Transport Partnership Group, - Air Subgroup Technical Expert Team)

Contents

6048

Chapter 3 Levels of Mercury in Air

3.1 Background

The aim of this chapter is to provide an up-to-date overview of mercury levels in air (since the GMA 2013). In particular, this chapter focuses on atmospheric mercury measurements and regional/worldwide spatial and temporal trends. The information presented here will include an overview of measurements currently collected in regional monitoring networks around the world. This chapter will also include an overview of high altitude and vertical profile measurements and mercury exchange fluxes at the air/water/soil/vegetation/snow-ice interfaces. A summary of new non-standard/conventional methods available (under development) for monitoring mercury in air is also be presented. The chapter will conclude with an overall assessment of the state of atmospheric mercury measurements and our current understanding of the state of the science.

Specifically, this chapter highlights recent key findings on:

- Atmospheric mercury measurements and trends worldwide and at the regional/continental scale with a focus on the spatial and temporal variability of Hg and its compounds concentrations at ground-based sites, at different altitudes and latitudes in the Southern and Northern Hemispheres.
- Atmospheric mercury in polar environment (Arctic and Antarctica) and the specific aspects related to these regions in terms of impact caused by Long Range Transport (LRT) and in-situ formation and transformation processes.
- Recent studies on vertical profile measurements over background regions and over impacted (industrial/urban) regions to support modelling uncertainty and advance our understanding of LRT and deposition/re-emission patterns.
- Temporal and spatial variability in Hg exchange fluxes between air and soil/vegetation/snow-ice interfaces, and also including contaminated sites (industrial, mining areas).
- Recent advances in monitoring applications using new/non-standard methods for measuring Hg species in the atmosphere.

3.2 Atmospheric mercury measurements and trends worldwide

3.2.1 Introduction

Atmospheric Hg is monitored in national programs driven by national legislation or international agreements and conventions. Extensive monitoring is also conducted as a part of long-term research programs. Many national networks operate in the context of international conventions or agreements and this cooperation also includes development of joint procedures both for measurements and reporting of data and for regular evaluation of trends and patterns. For example, in Europe, air monitoring data on Hg is reported to EMEP (The European Monitoring and Evaluation Programme) under the Convention on Long-range Transboundary Air Pollution (CLRTAP). Arctic countries report data to AMAP (The Arctic Monitoring and Assessment Program under the Arctic Council) and Asian/Pacific countries to APMMN (the Asia-Pacific Mercury Monitoring Network). National networks differ in terms of ambition level e.g. relating to sampling frequency and whether speciation of airborne mercury is included.

National monitoring can provide the basis and infrastructure for research programs where routine monitoring can be expanded to more advanced methodologies for e.g. speciation of airborne Hg, and also new sites in locations where measurement data were previously not available. Examples of programs contributing results to this chapter are the GMOS program and several research projects focussed on Polar regions. The GMOS network continues to operate many of the sites in coordination with national programs and regional agreements. Monitoring stations are located mostly at background sites in order to intercept major intercontinental and continental air mass transport patterns. Master sites provide atmospheric Hg measurement speciated data including total Hg in precipitation samples whereas secondary sites provide Total Gaseous Mercury (TGM) measurement data and total Hg in precipitation (see www.gmos.eu for further details).

According to data provided by Governments to UNEP within the 'Global Review of Mercury Monitoring networks' (UNEP, 2016), the national monitoring networks are reported in the Table 1.

Table 1: Global Review of mercury monitoring networks (UNEP, 2016).

National area	Program/ network/ inventory	Number of monitoring stations/ sites	Managing Institution	Main website
Andorra	Andorran Air Quality network	Not available	Department of Environment and Sustainability	
Australia	The Australian National Pollutant inventory (NPI)	Not available		https://data.gov.au/dataset/npi
Austria	Network for		Austrian Federal	Austrian Bio-indicator Grid

	Mercury impacts in forest foliage		Research Centre for Forests controls	
Brazil	Mercury monitoring Network	Not available	CETESB, the environmental agency of the State of São Paulo	http://www.cetesb.sp.gov.br/2014/10/27/cetesb-realiza-treinamentos-internacionais-sobre-pops-e-mercurio/
Canada	The Canadian Air and Precipitation Monitoring Network (CAPMoN) & others (including AMAP)	3 stat. for air meas..	CAPMoN	https://www.ec.gc.ca/rs-mn/default.asp?lang=En&n=6C2AD92E-1 **http://nadp.sws.uiuc.edu/**
		+7 stat. for air meas.	Environment Canada	
		+ 2 remote stat.	Canadian Northern Contaminants Program (NCP) – Environment Canada	
China (Taiwan)	Wet deposition Network	11 sampling sites + 1 remote site	Environmental Protection Administration	
European Union	Network under EU Directive 2004/107/EC		EEA	http://cdr.eionet.europa.eu/ https://www.eea.europa.eu/data-and-maps/data/aqereporting-2
Hungary	Hungarian Air Quality Monitoring Network	One sampling site	Hungarian Meteorological Service	
Korea		12 monitoring stations	National Institute of Environmental Research (NIER) in the Ministry of Environment	
Japan	2 Mercury Monitoring Networks	281 monitoring stations	National Institute for Minamata Disease (NIMD) and the National Institute for Environmental Studies (NIES)/Ministry of Environment (MOE).	
Poland	Polish State Environmental Monitoring programme	5 monitoring stations	Inspection of Environmental Protection	http://www.gios.gov.pl/en/state-of-the-environment/state-environmental-monitoring
Romania	Mercury Monitoring Network	Sites in 41 counties	Ministry of Environment, NEPA and the National Environmental Guard	
United Kingdom	National Metals Network and National Atmospheric Emission Inventory	2 monitoring stations	UK DEFRA	https://uk-air.defra.gov.uk/networks/network-info?view=metals http://naei.defra.gov.uk/overview/pollutants?pollutant_id=15
Vietnam	--------	1 monitoring station	Vietnamese Centre for Environmental Monitoring (CEM) of the Vietnam Environment Administration (VEA)	
Global network	GMOS	Several stations in both hemispheres	CNR-IIA Division of Rende, Italy	www.gmos.eu

Regional network	NADP	Several stations in USA, Canada	NADP Program Office Illinois State Water Survey, 2204 Griffith Drive Champaign, IL 61820-7495	http://nadp.sws.uiuc.edu/mdn/

6101
6102 The UNEP Review lists general information on existing national monitoring networks but doesn't include
6103 data on mercury concentrations and depositions.

6104 Figure 1 provides a global picture of major monitoring networks that are part of global and regional
6105 networks mentioned in several sections of this chapter. It shows that though we have monitoring sites
6106 in both hemispheres, but there are regions (even large regions) that are completely lucking of
6107 monitoring data/sites which makes the evaluation of current situation in terms of geospatial distribution
6108 (gradients and variability) of Hg concentration in ambient air not feasible to do.

6109

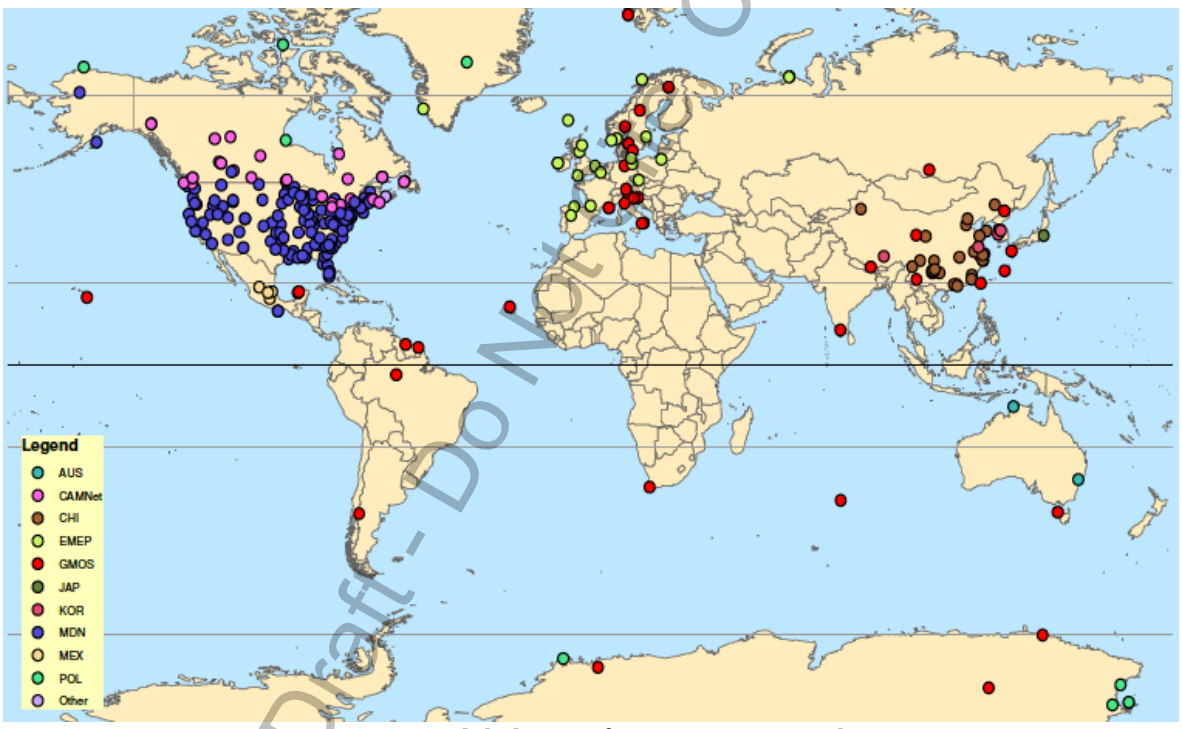

6110
6111 Figure 1 - Global map of monitoring networks

6112 ### 3.2.2 Spatial and temporal variability in the Southern and Northern Hemispheres

6113 Extensive measurements and data analysis have been performed across several ground-based sites as
6114 part of the GMOS program network. GMOS will continue its operation by providing support to site
6115 operators for online QA/QC and technical assistance as necessary through the Global Observation
6116 System on Mercury (GOS4M) that is one of the four flagships of GEO (Group on Earth Observation) and

will be financially supported through the ERA-PLANET (www.era-planet.eu) program. Tables 2 and 3 show annual values for speciated Hg concentrations at all sites from 2012 to 2014. In both Tables 1 and 2, the stations are ordered by latitude, thus describing the spatial atmospheric mercury variations moving from Northern to Southern Hemisphere. Mean GEM values of most of the sites located in the Northern Hemisphere were between 1.3 and 1.6 ngm^{-3},which is comparable to the concentrations measured at the long-term monitoring stations at Mace Head, Ireland (Ebinghaus et al., 2011; Slemr et al., 2011; Weigelt et al., 2015; Cole et al. 2014), and Zingst, Germany (Kock et al., 2005). In contrast, GEM concentrations from the EVK site, located at 5050 m above sea level in the Eastern Himalaya of Nepal, reported mean values below 1.3 ng m^{-3}. This value is comparable to free tropospheric concentrations measured in August 2013 over Europe (Weigelt et al., 2016). GEM concentration means observed at the stations in the Northern Hemisphere are also in good agreement with the overall mean concentrations observed at multiple sites in Canada (ranging from 1.23±0.37 to 3.75 ± 2.22 ng m^{-3} overall measurements collected from 1994-2011) (Cole et al., 2014) and those reported from 2 Arctic stations (VRS, PAL) (Sprovieri et al., 2016). Seasonal variations of GEM concentrations have also been observed at all European sites in the Northern Hemisphere, with most of them showing higher concentrations during the winter and spring and lower concentrations in summer and fall seasons.

Table 2: Annually averaged GEM mean concentrations from 2012 to 2014 at the GMOS stations (Sprovieri et al. 2016).

	Code	Site	Elev (m asl)	Lat	Lon	Country	2012 GEM Mean ± St.Dev. ($ng\ m^{-3}$)	2013 GEM Mean ± St.Dev. ($ng\ m^{-3}$)	2014 GEM Mean ± St.Dev. ($ng\ m^{-3}$)
Northern Hemisphere	VRS	Villum Research Station	30	81.58033	-16.60961	Greenland	1.44 ± 0.27	1.61 ± 0.41	1.41 ± 0.35
	PAL	Pallas	340	68.00000	24.23972	Finland	- ± -	1.45 ± 0.11	1.47 ± 0.17
	RAO*	Råö	5	57.39384	11.91407	Sweden	1.33 ± 0.20	1.43 ± 0.16	1.48 ± 0.23
	MHE	Mace Head	5	53.32511	-9.90500	Ireland	** ± **	1.46 ± 0.17	1.41 ± 0.14
	LIS	Listvyanka	670	51.84670	104.89300	Russia	- ± -	1.34 ± 0.38	1.39 ± 0.40
	CMA	Col Margherita	2545	46.36711	11.79341	Italy	- ± -	- ± -	1.69 ± 0.29
	MCH*	Mt. Changbai	741	42.40028	128.11250	China	- ± -	1.78 ± 0.48	1.57 ± 0.42
	LON*	Longobucco	1379	39.39408	16.61348	Italy	- ± -	1.43 ± 0.33	- ± -
	MWA	Mt. Walinguan	3816	36.28667	100.89797	China	- ± -	1.33 ± 0.64	1.31 ± 0.60
	MIN	**Minamata**	**20**	**32.23056**	**130.40389**	**Japan**	1.95 ± 0.48	1.86 ± 0.40	1.91 ± 0.40
	EVK	Ev-K2	5050	27.95861	86.81333	Nepal	1.14 ± 0.17	1.11 ± 0.42	1.33 ± 0.22
	CHE*	**Cape Hedo**	**60**	**26.86430**	**128.25141**	**Japan**	2.12 ± 0.47	1.74 ± 0.38	1.78 ± 0.35
	MAL	Mt. Ailao	2503	24.53791	101.03024	China	- ± -	2.04 ± 0.64	1.33 ± 0.40
Tropics	SIS	Sisal	7	21.16356	-90.04679	Mexico	- ± -	1.20 ± 0.24	1.11 ± 0.37
	CAL	Calhau	10	16.86402	-24.86730	Cape Verde	- ± -	1.22 ± 0.14	1.20 ± 0.09
	KOD	Kodaicanal	2333	10.23170	77.46524	India	- ± -	1.54 ± 0.20	1.54 ± 0.26
	NIK	Nieuw Nickerie	1	5.95679	-57.03923	Suriname	- ± -	1.13 ± 0.42	1.28 ± 0.46
	MAN*	Manaus	110	-2.89056	-59.96975	Brazil	- ± -	1.08 ± 0.23	0.99 ± 0.23
Southern Hemisphere	AMS*	Amsterdam Island	70	-37.79604	77.55095	Terres Australes et Antarctiques Françaises	1.03 ± 0.07	1.03 ± 0.09	1.05 ± 0.05
	CPT	Cape Point	230	-34.35348	18.48983	South Africa	1.07 ± 0.10	1.03 ± 0.11	1.09 ± 0.12
	BAR	Bariloche	801	-41.12873	-71.42010	Argentina	1.01 ± 0.11	0.89 ± 0.15	0.87 ± 0.15
	DDU	Dumont d'Urville	40	-66.66281	140.00292	Antarctica	0.91 ± 0.2	0.85 ± 0.19	0.86 ± 0.38
	DMC	Concordia Station	3220	-75.10170	123.34895	Antarctica	0.76 ± 0.24	0.84 ± 0.27	- ± -

*** to be included*

* *GMOS Master stations with speciation Hg data*

in bold External GMOS Partners

Table 3: Annually-averaged PBM and GOM mean concentrations from 2012 to 2014 at the GMOS stations (Sprovieri et al. 2016).

							2012		2013		2014	
	Code	Site	Elev (m asl)	Lat	Lon	Country	PBM Mean ± St.Dev. ($pg\,m^{-3}$)	GOM Mean ± St.Dev. ($pg\,m^{-3}$)	PBM Mean ± St.Dev. ($pg\,m^{-3}$)	GOM Mean ± St.Dev. ($pg\,m^{-3}$)	PBM Mean ± St.Dev. ($pg\,m^{-3}$)	GOM Mean ± St.Dev. ($pg\,m^{-3}$)
NH	RAO	Råö	5	57.39384	11.91407	Sweden	2.89 ± 3.27	0.63 ± 1.73	3.96 ± 3.77	0.54 ± 0.85	4.41 ± 5.87	1.25 ± 1.87
NH	MCH	Mt. Changbai	741	42.40028	128.11250	China	-	-	17.10 ± 14.25	4.96 ± 6.33	-	-
NH	LON	Longobucco	1379	39.39408	16.61348	Italy	-	-	3.28 ± 3.82	11.33 ± 29.90	-	-
NH	MWA	Mt. Waliguan	3816	36.28667	100.89797	China	-	-	98.59 ± 37.79	12.32 ± 6.33	-	-
NH	**CHE**	**Cape Hedo**	**60**	**26.86430**	**128.25141**	**Japan**	1.77 ± 2.46	1.10 ± 1.80	3.70 ± 3.60	1.46 ± 2.19	4.03 ± 5.25	2.26 ± 3.71
T	MAN	Manaus	110	-2.89056	-59.96975	Brazil	-	-	5.04 ± 4.13	1.72 ± 0.72	1.45 ± 1.81	1.61 ± 1.75
SH	AMS	Amsterdam Island	70	-37.79604	77.55095	Terres Australes et Antarctiques Françaises	1.76 ± 1.20	1.65 ± 0.82	2.05 ± 1.37	1.53 ± 0.45	2.22 ± 1.83	2.03 ± 1.44

Table 4 summarizes the summary of the annual wet deposition fluxes and the weighted THg concentrations observed at the 17 GMOS sites from the Northern, Tropical, and Southern Hemispheres between 2011 and 2015 (Sprovieri et al., 2017). Seasonal trend analysis of THg in precipitation showed increasing Hg concentrations and Hg deposition during the spring and summer months. However, the patterns of THg concentrations and precipitation amounts reveal that, at most of the sites, the seasonal THg wet deposition maximum corresponds to the maximum in precipitation amounts collected. The dominant factor in determining the Hg wet deposition loading recorded at all the European sites was then generally related to the amounts of the collected precipitation.

Table 4: Annual wet deposition fluxes [$\mu g m^{-2} yr^{-1}$] and weighted THg concentrations [$ng L^{-1}$] observed at GMOS stations from 2011 to 2015 (Sprovieri et al. 2017).

	Code	Station	Elev (m asl)	Lat	Lon	Country	2011		2012		2013		2014		2015	
							Annual Wet Dep. Flux [µg m^{-2} yr^{-1}]	Weighted HgT [ng L^{-1}]	Annual Wet Dep. Flux [µg m^{-2} yr^{-1}]	Weighted HgT [ng L^{-1}]	Annual Wet Dep. Flux [µg m^{-2} yr^{-1}]	Weighted HgT [ng L^{-1}]	Annual Wet Dep. Flux [µg m^{-2} yr^{-1}]	Weighted HgT [ng L^{-1}]	Annual Wet Dep. Flux [µg m^{-2} yr^{-1}]	Weighted HgT [ng L^{-1}]
Northern Hemisphere	NYA	Zeppelin	474	78.90806	11.88139	Norway	-	-	0.9	**3.8**	0.9	**4.1**	1.7	**5.7**	0.8	**4.4**
	PAL	Pallas	340	68	24.23972	Finland	2.9	**7.1**	1.9	**6.8**	1.3	**4.5**	2.3	**6.1**	-	-
	RAO	Råö	5	57.393835	11.914066	Sweden	5.8	**8.9**	6.5	**10.4**	4.2	**8.2**	6.3	**9.9**	-	-
	MHE	Mace Head	5	53.325106	-9.905	Ireland	-	-	0.9	**2.2**	4.8	**4.6**	4.1	**6.6**	-	-
	LIS	Listvyanka	670	51.8467	104.893	Russia	-	-	0.2	**9.7**	0.1	**2.6**	-	-	-	-
	CMA	Col Margherita	2545	46.36711	11.79341	Italy	-	-	-	-	-		4.4	**7.8**	-	-
	ISK	Iskrba	520	45.561217	14.858047	Slovenia	5.1	**7.5**	8.4	**6.2**	7.2	**5.3**	10.0	**6.1**	3.0	**3.0**
	MCH	Mt. Changbai	741	42.40028	128.11250	China	2.8	**10.6**	4.8	**8.4**	1.2	**3.9**	1.0	**5.4**	-	-
	LON	Longobucco	1379	39.39408	16.61348	Italy	-	-	0.3	**3.9**	3.1	**6.6**	-	-	-	-
	MWA	Mt. Waliguan	3816	36.28667	100.89797	China	-	-	0.3	**4.3**	0.4	**6.4**	2.2	**15.0**	-	-
	MAL	Mt. Ailao	2503	24.53791	101.03024	China	4.3	**2.8**	3.2	**3.3**	5.5	**5.3**	0.2	**6.7**	-	-
Tropics	SIS	Sisal	7	21.16356	-90.04679	Mexico	-	-	-	-	7.4	**11.0**	6.5	**9.1**	-	-
	CST	Celestun	3	20.85838	-90.38309	Mexico	-	-	2.4	**8.1**	0.1	**13.5**	-	-	-	-
Southern Hemisphere	AMS	Amsterdam Island	70	-37.79604	77.55095	Terres Australes et Antarctiques Françaises	-	-	-	-	1.95	**2.34**	1.55	**1.80**	-	-
	CPT	Cape Point	230	-34.35348	18.48983	South Africa	0.3	**2.1**	3.8	**14.6**	5.2	**19.6**	0.57	**1.84**	0.6	**3.0**
	CGR	Cape Grim	94	-40.683333	144.689444	Australia	-	-	-	-	3.1	**4.0**	3.8	**6.7**	3.1	**6.5**
	BAR	Bariloche	801	-41.12873	-71.42010	Argentina	-	-	-	-	-	-	0.1	**0.4**	0.5	**0.6**

3.2.1.1 Atmospheric Hg concentrations and pattern analysis in the Southern Hemisphere (SH)

For the sites located in the SH as part of GMOS network (see Table 2), mean GEM concentrations (~ 1.0 ngm^{-3}) are lower than those reported in the Northern Hemisphere (~ 1.5 ngm^{-3}) but are in good agreement with the previously reported southern hemispherical background levels (Sprovieri et al., 2010; Angot et al., 2014; Slemr et al., 2015) and the expected range for remote sites in this region. A small (within ~ 0.1 ngm^{-3}) seasonal variability in GEM concentrations was observed at Cape Point and Amsterdam Island with highest values during austral winter and lowest values in summer (Slemr et al., 2015) but the variability in concentrations is much lower than in the Northern Hemisphere. GEM concentrations are comparable at all SH monitoring sites, whereas the lower concentrations of GEM observed (<1ngm^{-3}), were associated with air masses coming from the southern Indian Ocean and the Antarctic continent (Angot et al., 2014).

3.2.1.2 Wet deposition at Tropical Sites and in the SH

Hg deposition measurements are scarce in tropical latitudes; hence there have been few scientific publications within the past decade from this region (Shanley et al., 2015 and references therein). The tropics are a particularly important region with regard to global atmospheric chemistry and 49% of total Hg(II) deposition globally occurs in the tropical oceans (Horowitz et al., 2017). Due to intense ultraviolet radiation and high water-vapour concentrations, high OH concentrations oxidize inorganic and organic gases, and induce an efficient removal from the atmosphere of the oxidized products. To address the

regional gap of information, the GMOS program initiated Hg deposition measurements in Mexico at Sisal station (see Table 3). High wet Hg deposition flux at this site suggested that other tropical areas maybe hotspots for Hg deposition as well. A number of studies have suggested that this could be due to higher precipitation and the scavenging ratios from the global pool in the subtropical free troposphere where high concentrations of oxidized Hg species exist (Selin and Jacob, 2008). These findings were also highlighted in previous studies in the south of Florida and the Gulf of Mexico coastal areas, confirming that local and regional Hg emissions play only a minor role in wet Hg deposition (Sillman et al., 2013) and suggesting that the primary source of scavenged oxidized Hg could be the global pool. In remote areas such as the Southern Hemisphere, far from any local sources, atmospheric deposition has been recognized as the main source of Hg to the ocean (Lindberg et al., 2007; Pirrone et al., 2008; Sunderland and Mason, 2007). Total mercury (THg) exhibited annual and seasonal patterns in Hg wet deposition samples. Inter-annual differences in total wet deposition are mostly linked with precipitation volume, with the greatest deposition flux occurring in the wettest years (see Table 4) (Sprovieri et al., 2017).

3.2.2 Spatial and temporal variability in U.S.A.

3.2.2.1 NADP's Mercury Deposition Network

The National Atmospheric Deposition Program's Mercury Deposition Network (MDN) makes long-term measurements of mercury in precipitation (wet deposition) across North America. The MDN began monitoring in 1996. The MDN sites follow standard procedures, and uniform precipitation collectors and rain gages to make weekly-integrated measurements of total mercury in a combined precipitation measurement (wet only) from Tuesday to Tuesday. Some daily samples are available. Sample bottles are pre-charged with acid to preserve the mercury sample. Currently, the MDN has 106 active sites. All MDN samples are analysed for total mercury concentration using Cold Vapour Atomic Florescence Spectroscopy (CVAFS). Invalid samples are identified using standard protocols. Subsamples for some sites are analysed for methyl mercury (MeHg). Valid and invalid results are provided for use by the scientific community (http://nadp.isws.illinois.edu/ mdn/).

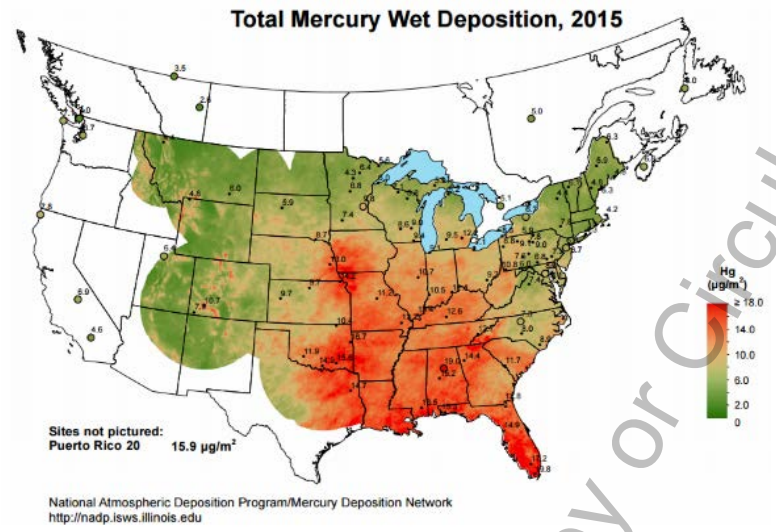

Figure 2: Total mercury wet depositions recorded in North America (2015). All years available at http://nadp.isws.illinois.edu

	Mercury Concentrations (ng/L)		
Year	N valid obs.	PW Mean	Median
2010	4,495	8.51	6.33
2011	4,286	9.01	6.99
2012	4,357	9.15	7.03
2013	4,391	9.02	7.17
2014	4,848	8.83	6.98
2015	4,798	8.04	6.4

All observations are used to determine total mercury deposition over North America in annual maps of precipitation weighted mean concentration (ng/L) and flux (ug/m^2 year, see figure). Precipitation-weighted average concentrations for 2015 are shown in the nearby Figure (??), and annual basic statistics are provided in the Table 5 (??).

Over the MDN measurement area, significant wet deposition is found along the U.S. Gulf Coast, and somewhat inland. Wet mercury deposition in these areas strongly correlates with higher precipitation (40-60 inches per year or >1000 cm/year). This pattern is repeated annually. Highest concentrations are found in the western areas where precipitation is lowest, and dominated by winter snow.

Trends over time in MDN data have been investigated by several research groups (Butler et al., 2008; Prestbo and Gay, 2009; Risch et al., 2012; Weiss-Penzias et al., 2016). Evaluating data through the mid 2000s, Butler et al. showed general decreases in eastern U.S. concentrations, with significant decreases

at about half of these sites. Fewer significant trends were seen in the Southeast, but the general tendency was for decreasing concentrations. Prestbo and Gay found significant decreasing concentration trends at about half of the sites (mostly in the East), particularly across Pennsylvania and extending up through the Northeast, and fully consistent with Butler et al. Two sites in the West (Colorado, Washington) showed the same decreases. No significant concentration increases were noted, with little change in the Upper Midwest concentration or deposition. Risch et al., focusing on the Great Lakes region, found only "small localized decreases" in Hg concentration. Deposition trends were present, but not at these same sites; Overall, mercury deposition in the Great Lakes area remained unchanged between 2002 and 2008.

Weiss-Penzias et al reported wet concentrations almost exclusively decreasing between 1997 and 2013, with over 50% of the MDNsites showing significant decreases (of 19 sites). However, for the time period 2007–2013 (with 71 sites), increasing concentrations were just as numerous as decreasing concentrations, and this increased with one shorter time period, and positive tendencies were wide spread. Regional trend analyses revealed significant positive trends in Hg concentration in the Rocky Mountains, Plains, and Upper Midwest regions for the more recent time periods.

3.2.2.2 NADP's Atmospheric Mercury Network

The NADP's Atmospheric Mercury Network (AMNet) measures atmospheric mercury that contributes to mercury deposition using automated, continuous measurement systems, and standardized methods. Currently, there were 21 AMNet sites, and data from the AMNet are available on the NADP website (http://nadp.isws.illinois.edu/ amn). AMNet observations have been made since 2009 and are made continuously (five-minute and two-hour averages).

Network	Year	Mercury in Precipitation (wet deposition)				
NADP's MDN		Species	Valid Observations	PW Mean	Median	Units
	2010	total mercury	4,495	8.51	6.33	ng/L
	2011		4,286	9.01	6.99	ng/L
	2012		4,357	9.15	7.03	ng/L
	2013		4,391	9.02	7.17	ng/L
	2014		4,848	8.83	6.98	ng/L
	2015		4,798	8.04	6.4	ng/L

Table 2

		Atmospheric Mercury Concentrations	Valid Observations	Mean	Median	Units
NADP's AMNet	2010	GEM	51,289	1.57	1.43	ng/m3
		GOM	38,744	6.5	1.39	pg/m3
		PBM	38,099	6.67	3.78	pg/m3
	2011	GEM	54,541	1.59	1.44	ng/m3
		GOM	44,864	15.92	1.35	pg/m3
		PBM	44,817	8.23	4.09	pg/m3
	2012	GEM	42,924	1.47	1.42	ng/m3
		GOM	36,226	19.74	1.22	pg/m3
		PBM	37,386	13.13	4.18	pg/m3
	2013	GEM	39,078	1.49	1.44	ng/m3
		GOM	30,806	14.35	1.29	pg/m3
		PBM	30,919	10.33	4.45	pg/m3
	2014	GEM	49,348	1.47	1.4	ng/m3
		GOM	35,390	12.64	1.52	pg/m3
		PBM	35,238	10.99	4.96	pg/m3
	2015	GEM	52,938	1.58	1.38	ng/m3
		GOM	44,179	12.47	1.59	pg/m3
		PBM	43,022	8.62	4.11	pg/m3

6260 Data are qualified and averaged to one-hour (GEM in ng m^{-3}) and two-hour values (GOM, and $PBM_{2.5}$, in
6261 pg m^{-3}).

6262 Valid data are released for use by the scientific community, and also released in annual figures of
6263 mercury variability for sites meeting certain criteria. Annual average statistics are shown in the Table 5.

6264 The median GEM concentration found in the network is 1.38 ng/m3, and varies somewhat across the
6265 network. However, larger differences were present between sites for GOM and PBM concentrations in
6266 AMNet. GOM concentrations are generally higher in the urban environment, with lowest concentrations
6267 along the Pacific Ocean and other coastal sites. $PBM_{2.5}$ concentrations measured were generally the
6268 same as with GOM. The occurrence of very high outlier concentrations were noted at almost all of the
6269 sites (figure).

6270 Investigations of AMNet trends over time are currently ongoing.

6271 **Table 5:** Annual average statistics……(title TO BE COMPLETED)

	Atmospheric Mercury Concentrations	Valid Observations	Mean	Median	Units
2010	GEM	51,289	1.57	1.43	ng/m3
	GOM	38,744	6.5	1.39	pg/m3
	PBM	38,099	6.67	3.78	pg/m3
2011	GEM	54,541	1.59	1.44	ng/m3
	GOM	44,864	15.92	1.35	pg/m3
	PBM	44,817	8.23	4.09	pg/m3
2012	GEM	42,924	1.47	1.42	ng/m3
	GOM	36,226	19.74	1.22	pg/m3
	PBM	37,386	13.13	4.18	pg/m3
2013	GEM	39,078	1.49	1.44	ng/m3
	GOM	30,806	14.35	1.29	pg/m3
	PBM	30,919	10.33	4.45	pg/m3
2014	GEM	49,348	1.47	1.4	ng/m3
	GOM	35,390	12.64	1.52	pg/m3
	PBM	35,238	10.99	4.96	pg/m3
2015	GEM	52,938	1.58	1.38	ng/m3
	GOM	44,179	12.47	1.59	pg/m3
	PBM	43,022	8.62	4.11	pg/m3

6272

6273

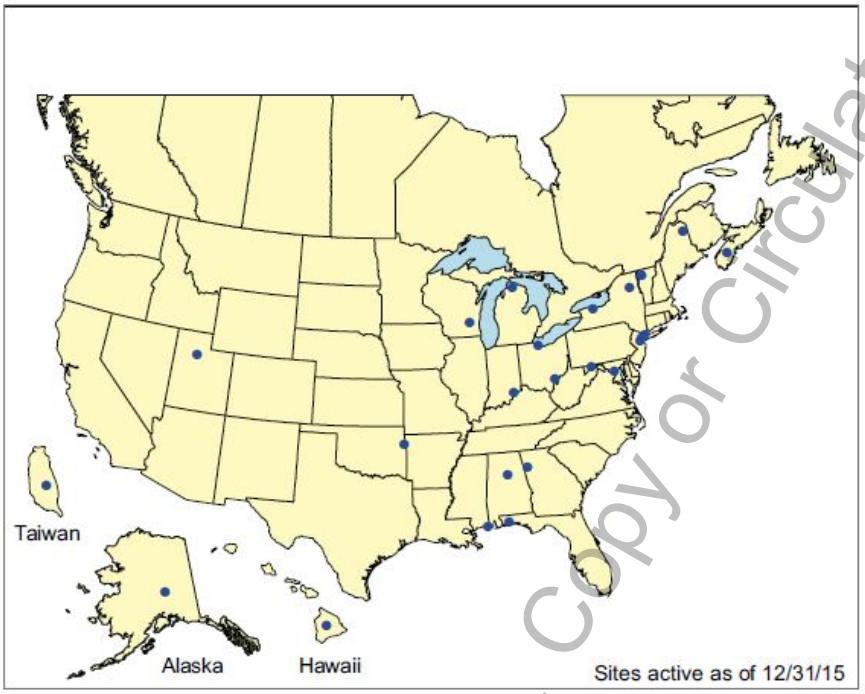

AMNet sites as of 12/31/2015.

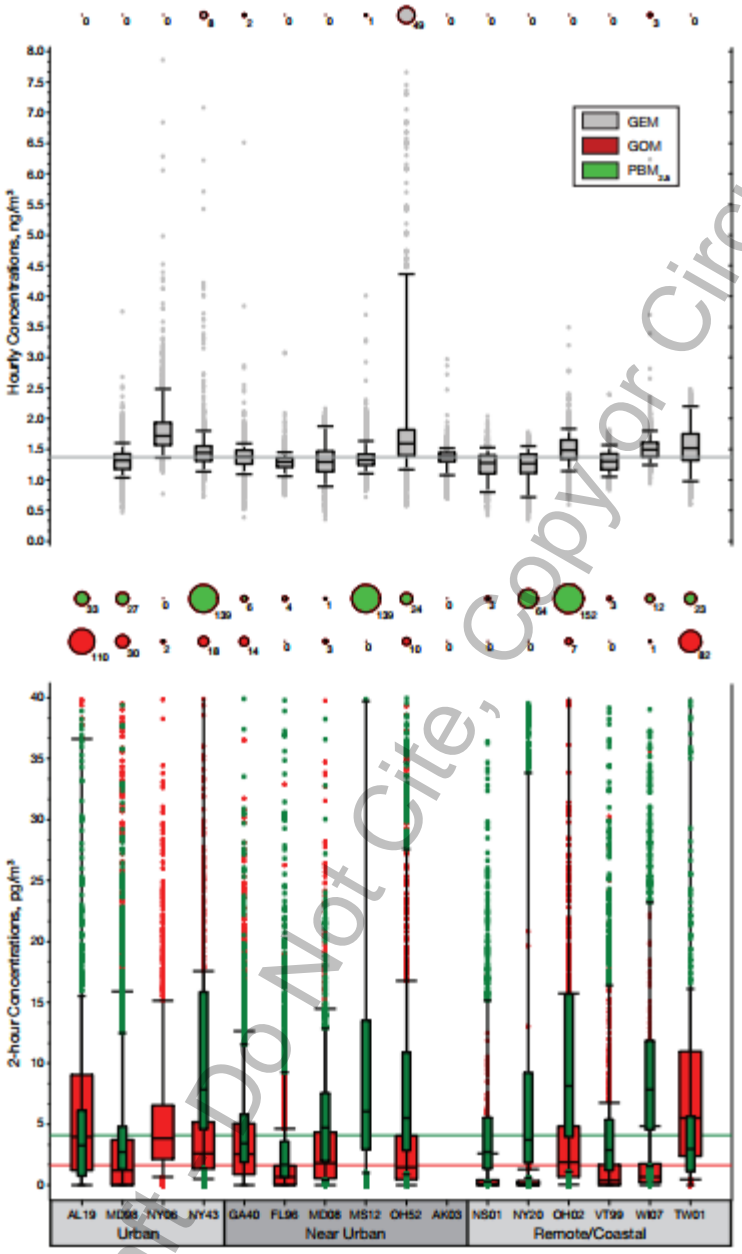

Figure @@: Hourly GEM concentrations in ng/m3 for each AMNet site (top) and 2-hour GOM and PBM2.5 concentrations in pg/m3 for each AMNet site (bottom), 2015. The bubble charts indicate the number of valid observations for GEM values above 8 ng/m3 , and GOM and PBM2.5 above 40 pg/m3 , the upper limit shown with the box plots. Horizontal lines in each graph represent the respective 2015 median values. From NADP, 2016.

Reference: National Atmospheric Deposition Program, 2016. National Atmospheric Deposition Program 2015 Annual Summary. NADP Data Report 2016-02. Illinois State Water Survey, University of Illinois at Urbana-Champaign, IL.

3.2.3 Canadian Atmospheric Mercury Network

Since 1994, considerable atmospheric Hg monitoring and research has taken place across Canada through both ongoing networks and independent research programs. Over time, the parameters measured have evolved, and the breadth and volume of data collected are significant. Most monitoring began as independent research programs to measure total gaseous mercury (TGM) in the early 1990s. Realizing the benefits of a community, researchers joined forces to create the Canadian Atmospheric Mercury Measurement Network (CAMNet) in 1994. CAMNet was operated by Environment and Climate Change Canada (ECCC) from 1994 to 2007, with between 7 and 15 sites across Canada. Later, some of these sites were transferred to the Canadian Atmospheric and Precipitation Monitoring Network (CAPMoN), which still operates these sites today and to other networks. The remainder of the currently operated ECCC sites are either part of the Northern Contaminants Program (NCP) or are run as part of ECCC measurement programs. As of 2017, these individual programs have been consolidated and fall under **Environment and Climate Change Canada – Atmospheric Mercury Monitoring or ECCC-AMM**. Table 6 shows all the atmospheric mercury measurements that have been taken across Canada. Figure XX shows the time periods from each site what measurements were made. Currently, there are 12 sites in Canada that collect continuous TGM and are highlighted in grey. In 1996, the United States-led Mercury Deposition Network (MDN) began collecting wet deposition samples for total mercury (THg) and, at some sites, methyl mercury (MeHg). Canada has joined forces with the MDN and has had up to 18 precipitation monitoring sites operating as part of the network over time. The sites where these precipitation measurements have been made over time are listed in Table XX. Currently, there are 7 sites in Canada that collect wet deposition measurements of mercury and are highlighted in grey. Finally, during the early 2000s, to meet increasing research needs, considerable advancements were made in instrument capabilities to collect and analyse mercury species in the air. From 2002 onward, some CAMNet sites began continuous measurements that could distinguish among gaseous elemental mercury (GEM), reactive gaseous mercury (RGM) and particulate mercury (TPM) (termed speciated atmospheric mercury). The sites which have made these measurements over time are listed in Table 6. Currently, there are 6 sites in Canada that collect continuous termed speciated atmospheric mercury and are highlighted in grey. As of January 2017, The ECCC-AMM monitors TGM at 12 sites, atmospheric speciated mercury at 6 sites and wet deposition at 5 sites. Figure 3 shows a map of the ECCC-AMM sites.

6321 **Table 6:** Mean concentrations of mercury data collected in Canada. The location of each site and the
6322 previous network or program under which the data was collected.

Station	Long (°W) Lat (°W)	Measurement period TGM	Mean TGM (ng m^{-3})	Measurement period Speciated Hg	Mean GEM (ng m^{-3})	Mean RGM (pg m^{-3})	Mean PHg (pg m^{-3})	Measurement period wet deposition	Mean Total Hg (ng L^{-1})
Little Fox Lake YK [a,g]	135.63 61.35	Jun 2007 – Oct 2011	1.28	-	-	-	-	-	-
Ucluelet BC [b]				-	-	-	-	-	-
Reifel Island BC [c, d]	123.17 49.10	Mar 1999 – Feb 2004	1.67	-	-	-	-	-	-
Saturna BC [c, d, e]	123.13 48.78	Mar 2009 – Dec 2010	1.43	-	-	-	-	Sep 2009 – Jan 2011	4.5
Whistler BC [b]	122.93 50.07	Aug 2008 – Oct 2011	1.21	-	-	-	-	-	-
Fort Vermilion AB [f]	116.02 58.38	-	-	-	-	-	-	Dec 2006 – Jan 2008	4.3
Meadows AB	114.64 53.53	May 2005 – Dec 2008	1.51	-	-	-	-	-	-
Genesee AB [b,d]	114.20 53.30	Mar 2004 – Dec 2010	1.53	Jan - Sep 2009	1.4	5.0	4.5	Jul 2006 – Jan 2011	12.8
Crossfield AB [f]	114.00 51.29	-	-	-	-	-	-	May 2006 – Dec 2007	9.3
Fort Chipewyan AB [c]	111.12 58.78	Jun 2000 – July 2001	1.36	-	-	-	-	-	-
Henry Kroeger AB [d]	110.83 51.42	-	-	-	-	-	-	Oct 2004 – Jan 2011	11.7
Esther AB [d, e]	110.20 51.67	Jun 1998 – Apr 2001	1.65					Apr 2000 – May 2001	14.2
Fort McKay South AB [h]	111.64 57.15	Aug 2013 – Dec 2016		Aug 2013 – Dec 2016				-	-
Patricia McInnis AB [h]	111.48 56.75	Oct 2010 – Dec 2016		-	-	-	-	-	-
Bratt's Lake SK [d,e]	104.71 50.20	May 2001 – Dec 2010	1.44	-	-	-	-	Jun 2001 – Jan 2011	11.2
Flin Flon MB [b]	101.88 54.77	Jul 2008 – Jun 2011	3.75	Jul 2010 – Mar 2011	2.06	3.4	10.4	Sep 2009 – Dec 2010	59.9
Churchill MB [f, i]	94.07 58.75	-	-	Mar – Apr 2004	1.52	100.9	168.5	Jun 2006 – Dec 2007	5.3
ELA ON [d,e,i]	93.72 49.66	-	-	May 2005 – Dec 2010	1.4	3.7	6.5	Nov 2009 – Jan 2011	9.6
Dorset ON [d, j, k]	78.93 45.22	-	-	Jul 2008 – Mar 2010	1.38	2.7	5.9	Jan 1997 – Dec 1998	9.7
Windsor ON [l]	83.01 42.18	Jan 2007 – Dec 2008	1.93	-	-	-	-	-	-
Burnt Island ON [c]	82.95 45.81	May 1998 – Dec 2007	1.55					Nov 2001 – Mar 2003	9.2
Mississauga ON [k]	79.65 43.54			Jan – Dec 2009	1.4	3.7	6.5		
Egbert ON [c,d,e]	79.78 44.23	Dec 1996 – Dec 2010	1.58	-	-	-	-	Mar 2000 – Jan 2011	8.4
Buoy ON [c]	79.45	Jul – Sep 2005	1.70	-	-	-	-	-	-

	43.40								
Kuujjuarapik QC [c]	77.73 55.30	Aug 1999 – Sep 2009	1.68	-	-	-	-	-	-
Point Petre ON [c]	77.15 43.84	Nov 1996 – Dec 2007	1.75	-	-	-	-	Nov 2001 – Mar 2003	9.1
Chapais QC [d,e]	74.98 49.82	-	-	-	-	-	-	Dec 2009 – Jan 2011	6.4
St. Anicet QC [b,c,d]	74.03 45.20	Aug 1994 – Dec 2009	1.60	Jan 2003 – Dec 2010	1.52	3	17.5	Apr 1998 – Aug 2007	7.9
St. Andrews NB [c,d]	67.08 45.08	Jan 1996 – Jul 2007	1.38	-	-	-	-	Jul 1996 – Dec 2003	6.6
Kejimkujik NS [c,d,e]	65.21 44.43	Jan 1996 – Dec 2010	1.40	Jan 2009 – Dec 2011	1.34	0.5	4.2	Jul 1996 – Jan 2011	5.2
Halifax NS [b]	63.67 44.67			Oct 2009 – Dec 2011	1.68	2.1	2.3		
Mingan QC [b,c]	64.17 50.27	Jan 1997 – Dec 2000	1.57	-	-	-	-	Apr 1998 – Aug 2007	5.0
Southampton PE [c]	62.58 46.39	Jan 2005 – Dec 2006	1.23	-	-	-	-	-	-
Alert NU [a]	62.33 82.50	Jan 1995 – Dec 2011	1.51	Jan 2002 – Dec 2011	1.26	21.8	41.1	-	-
Stephenville NL [d,e]	58.57 48.56	-	-	-	-	-	-	Feb 2010 – Jan 2011	5.6
Cormak NL [d,e]	57.38 49.32	-	-	-	-	-	-	May 2000 – Jul 2010	4.2

Legenda: a) Northern Contaminants Program (NCP); b) Clean Air Regulatory Agenda Mercury Science Program (CARA) currently Climate Change and Air Pollution program (CCAP); c) Canadian Atmospheric Mercury Measurement Network (CAMNet); d) The Mercury Deposition Network (MDN); e) The Canadian Air and Precipitation Monitoring Network (CAPMoN); f) Geological Survey of Canada (GSC); g) Intercontinental Atmospheric Transport of Anthropogenic Pollutants to the Arctic (INCATPA); h) Joint Oil Sands Monitoring Program (JOSM); i) University of Alberta; j) Ontario Ministry of the Environment (MOE); k) University of Toronto; l) University of Windsor. Long = Longitude; Lat = Latitude.

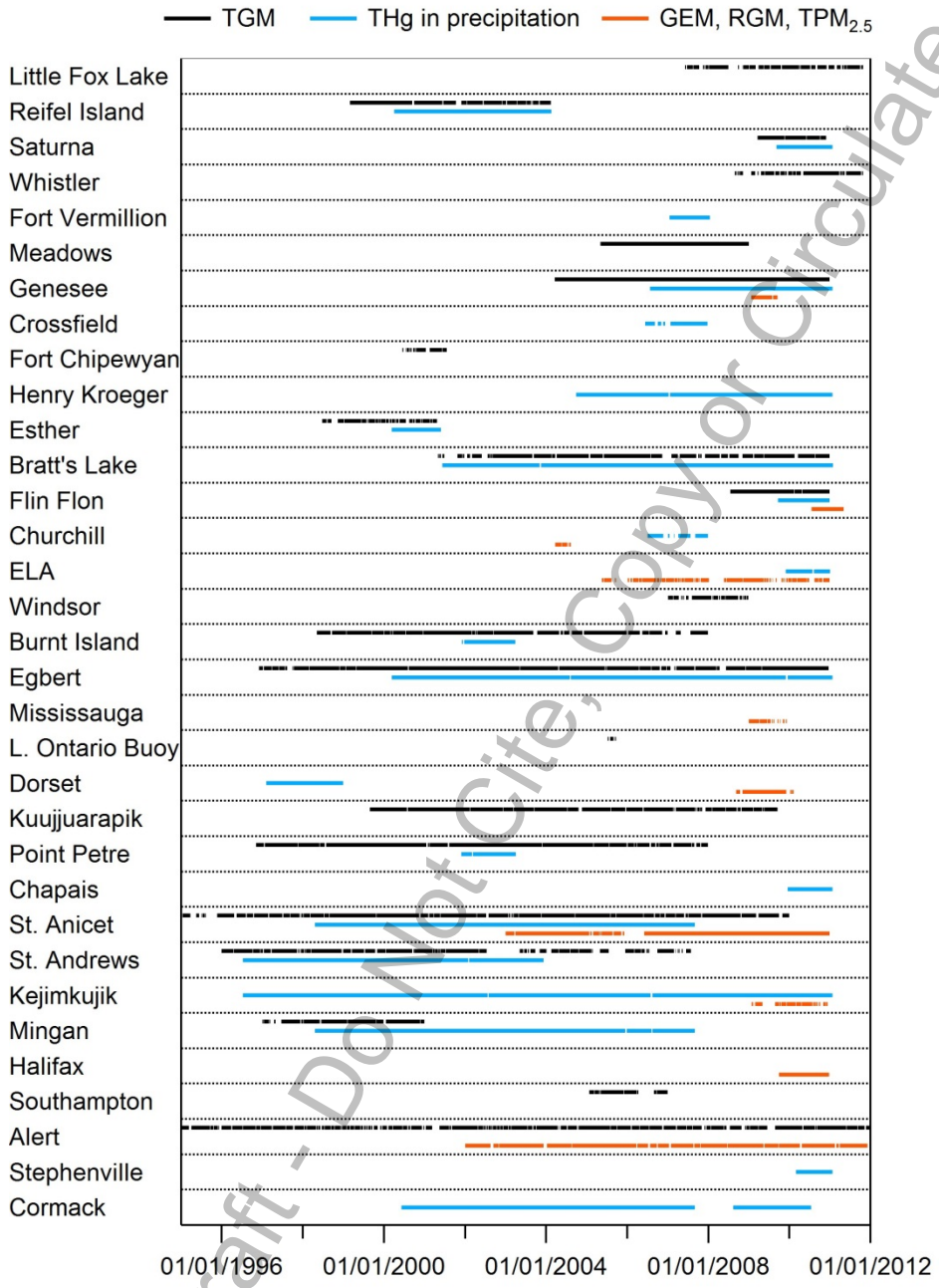

Figure 2: Time period of mercury measurements at Canadian monitoring sites

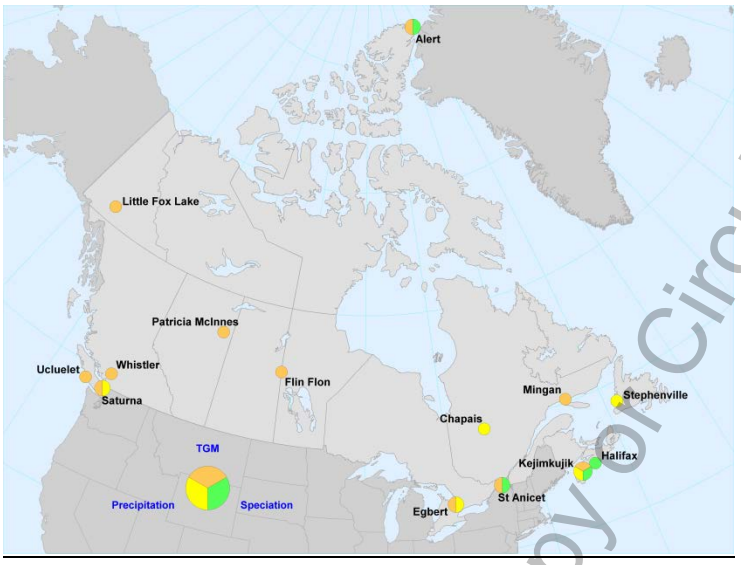

Figure 3: Environment and Climate Change Canada – Atmospheric Mercury Monitoring sites currently operating in Canada as of January 2017.

Trends of mercury over time have been investigated for many Canadian measurement sites for all 3 atmospheric mercury parameters including TGM, speciated mercury and mercury in precipitation (Cole et al., 2014). A minimum of 5 yr. of data were required to perform the trend analysis. The time period over which data are reported differs for each location. As a result, linear trends were estimated for all available data from each site rather than limiting the analysis to only overlapping time periods. Trends were calculated using the seasonal Kendall test for trend and the related Sen's slope calculation (Gilbert, 1987; van Belle and Hughes, 1984). This method is an extension of the non-parametric Mann-Kendall test for trend, which is recommended when there are missing values and when the data are not normally distributed; both of these conditions apply to these datasets.[1] Table XX summarizes the calculated trends of mercury in Canada over time for data sets that fall within the above parameters. The areas shaded in blue are currently operated sites in Canada.

[1] In the seasonal Kendall method, data from the 12 months are treated as 12 separate datasets. For each month, the presence of a trend is confirmed or rejected by the Mann-Kendall test, and a slope is estimated using Sen's nonparametric estimator of slope. An overall annual trend is estimated from the monthly trend statistics; however, this estimate may be questionable if the monthly trends are not homogeneous. Thus, to ensure reliability of the data, a test for seasonal homogeneity was performed as well. If seasonal trends were homogeneous, the results were used to determine an overall trend for the entire period. If they were not homogeneous, or when there was insufficient data in certain months, only trends for individual months were reported. The disadvantage of this technique is that it produces a linear trend over the entire period and can miss complex patterns such as a decrease followed by an increase.

Station	Measurement period TGM	Trend TGM (% yr^{-1})	Measurement period GEM/RGM/PHg	Trend GEM	Trend RGM	Trend PHg	Measurement period wet deposition	Trend Total Hg in precip
Little Fox Lake YK	Jun 2007 – Oct 2011		-	-	-	-	-	-
Ucluelet BC			-	-	-	-	-	-
Reifel Island BC	Mar 1999 – Feb 2004	-3.3 (-4.2 to -2.4)	-	-	-	-	-	-
Saturna BC	Mar 2009 – Dec 2010		-	-	-	-	Sep 2009 – Jan 2011	
Whistler BC	Aug 2008 – Oct 2011		-	-	-	-	-	-
Genesee AB	Mar 2004 – Dec 2010	-0.4 (ns) (-1.4 to +0.1)	-	-	-	-	Jul 2006 – Jan 2011	
Fort McKay South, AB			-	-	-	-	-	-
Patricia McInnis AB	Oct 2010 – Dec 2016		-	-	-	-	-	-
Henry Kroeger AB	-	-	-	-	-	-	Oct 2004 – Jan 2011	-
Bratt's Lake SK	2001 – 2010	-2.5 (-3.4 to -1.6)	-	-	-	-	-	-
Flin Flon MB	Jul 2008 – Jun 2011		-	-	-	-	-	-
ELA ON	-	-	May 2005 – Dec 2010	-	-	-	-	-
Burnt Island ON	1998 –2007	-2.5 (-3.4 to -1.6)		-	-	-	-	-
Egbert ON	1996 – 2010	-1.3 (-1.7 to -1.0)	-	-	-	-	2000-2010	-2.1 (-3.7 to -0.6)
Point Petre ON	1996 – 2007	-1.7 (-2.2 to -1.2)	-	-	-	-	-	-
Chapais QC	-	-	-	-	-	-	Dec 2009 – Jan 2011	
St. Anicet QC	1995 – 2009	-1.5 (-1.8 to -1.2)	Jan 2003 – Dec 2010				1998 – 2007	-3.7 (-6.5 to -0.3)
St. Andrews NB	1996 - 2007	-1.0 (-1.4 to -0.5)	-	-	-	-	Jul 1996 – Dec 2003	-
Kejimkujik NS	1996 – 2010	-0.9 (-1.1 to -0.6)	Jan 2009 – Dec 2011				1996 – 2011	-2.2 (-3.5 to +0.3)

Table 7 Annual trends over time of mercury data collected in Canada

2.2.4 Atmospheric mercury in Asia

Before the establishment of the GMOS global network independent programs and networks for monitoring atmospheric Hg species and deposition have been developed in Asia, such as those in Korea, Japan, China, and Chinese Taiwan supported by the National Science Foundation in each of the Asian countries and region. Since 2010, some of these Asian sites have been incorporated within the global network (Sprovieri et al., 2016), including Mt. Waliguan, Mt. Ailao, Shangri-La and Mt. Changbai in mainland China, Lulin in Chinese Taiwan, Cape Hedo, Okinawa and Minamata, Kyushu islands in Japan, Kanghwa Island in Korea, and Kodaikanal in India. A statistical summary of speciated atmospheric Hg concentrations and associated site information (urban and remote areas) in Asia is shown in Table 8 whereas Table 9 reports Hg concentrations and deposition fluxes in precipitation, throughfall, and

litterfall. GEM and PBM concentrations recorded at remote Chinese sites are elevated compared to that observed at background/remote areas in Europe and North America, and at others sites in the Northern Hemisphere (Sprovieri et al., 2016; Fu et al., 2015). In Chinese urban areas, the highly elevated GEM, GOM and PBM were mainly derived from local anthropogenic Hg emissions, whereas regional anthropogenic emissions and long-range transport from domestic source regions are the primary causes of the elevated GEM and PBM concentrations at remote sites (Fu et al., 2015). Mean GOM concentrations at remote sites in China ranged from 2.2 to 10.1 pgm^{-3}, significantly lower than those observed in the Chinese urban areas but comparable to the values in Europe and North America (Fu et al., 2015; Table 4).

Wet-only deposition fluxes of THg and MeHg ranged between 1.8–7.0 $\mu gm^{-2}\ yr^{-1}$ and 0.01–0.06 $\mu gm^{-2}yr^{-1}$, respectively, at remote sites, and 13.4-56.5 $\mu g\ m^{-2}\ yr^{-1}$ and 0.05–0.28 $\mu g\ m^{-2}\ yr^{-1}$ at urban sites, respectively. Wet deposition fluxes of THg and MeHg at urban sites in China were higher compared to those in North America and Europe, but wet deposition fluxes of THg at remote sites were in the lower range of those observed in North America and Europe. Regarding the Chinese GMOS sites, details on THg recorded from 2011 to 2015 are reported in Table 9.

Table 8: Atmospheric Hg concentrations at ground-based stations in Asia (Fu et al., 2015).

Site	Country	Elev (m asl)	Lat	Lon	Type	Study period	TGM or GEM Mean ± St.Dev. ($ng\ m^{-3}$)	PBM/TPM Mean ± St.Dev. ($pg\ m^{-3}$)	GOM Mean ± St.Dev. ($pg\ m^{-3}$)	Reference
An-myun	Korea	45.7	36.533°N	126.317°E	Background	12/2004-04/2006	4.61 ± 2.21	-	-	Nguyen et al. (2007)
Beijing	China	48	38.898° N	116.392° E	Urban	02&09/1998	10.40 ± 3.25	-	-	Liu et al. (2002)
						01-12/2006	-	272	-	Schleicher et al. (2015)
							-	573 ± 551*	-	
Cape Hedo	Japan	60	26.864° N	128.251° E	Background	01/2011-03/2015	1.91 ± 0.48	3.17 ± 4.41	1.89 ± 3.16	Sprovieri et al. (2016a)
Changchun	China	270	43.824° N	125.319° E	Urban	-/2001	18.4	276*	-	Fang et al. (2004)
Chemgshantou	China	30	37.38° N	122.68° E	Remote coast	07&10/2007, 01&04/2009	2.31 ± 0.74		-	Ci et al. (2011)
Chongming Island	China	11	31.522° N	121.908° E	Remote coast	9/12/2009	2.50 ± 1.50	-	-	Dou et al. (2013)
Chongqing	China	350	29.6° N	106.5° E	Urban	08/2006-09/2007	6.74 ± 0.37	-	-	Yang et al. (2009)
Guangzhou	China	60	23.124° N	113.355° E	Urban	11/2010-10/2011	4.60 ± 1.60	-	-	Chen et al. (2013)
Guiyang	China	1040	26.57°N	106.72° E	Urban	11/2011-11/2012	8.40 ± 4.87	-	-	Feng et al. (2004)
						12/2009-11/2010	10.2 ± 7.06	-	-	Fu and Feng (2015)
						08-12/2009	9.72 ± 10.2	368 ± 276	35.7 ± 43.9	Fu et al. (2011)
Jeju Island	Korea	60	33.283°N	120.167°E	Remote coast	05/2006-05/2007	3.85 ± 1.68	-	-	Nguyen et al. (2010)
Jiaxing	China	10	30.833° N	120.7° E	Urban	09/2005	5.40 ± 4.10	-	-	Wang et al. (2007)
Lanzhou	China	1540	36.067° N	103.79° E	Urban	-/2004	28.6	-	-	Su et al. (2007)
						04&07&10&12/1994	-	955*	-	Duan and Yang (1995)
Lulin	Chinese Taipei	2862	23.51°N	120.92° E	Background	04/2006-12/2007	1.73 ± 0.61	2.3 ± 3.9	12.1 ± 20.0	Sheu et al. (2010)
Minamata[T]	Japan	20	32.231°N	130.403° E	Rural	04/2011-12/2014	1.89 ± 0.43	-	-	Sprovieri et al. (2016a)
Miyun	China	220	40.481°N	116.775° E	Remote forest	12/2008-11/2009	3.22 ± 1.94	98.2 ± 113	10.1 ± 18.8	Zhang er al. (2013)
Mt. Ailao	China	2450	24.533°N	101.017° E	Remote forest	05/2011-05/2012	2.09 ± 0.63	31.3 ± 28.0	2.2 ± 2.3	Zhang et al. (2015b)
Mt. Changbai	China	740	42.402°N	128.112° E	Remote forest	10/2008-10/2010	1.60 ± 0.51	-	-	Fu et al. (2012b)
						07/2013-07/2014	1.73 ± 0.48	18.9 ± 15.6	5.7 ± 6.8	Fu et al. (2014)
Mt. Damei	China	550	29.632°N	121.565° E	Remote forest	04/2011-04/2013	3.31 ± 1.44	154 ± 104	6.3 ± 3.9	Yu et al. (2015)
Mt. Dinghu	China	700	23.164°N	112.549° E	Remote forest	09/2009-04/2010	5.07 ± 2.89	-	-	Chen et al. (2013)
Mt. Gongga	China	1640	29.649° N	102.117° E	Remote forest	05/2005-07/2007	3.98 ± 1.62	30.7 ± 32.0*	6.2 ± 3.9	Fu et al. (2008)
Mt. Jiuxian	China	1700	25.71° N	118.11° E	Remote forest	11/2010. 01&04&08/2010	-	24.0 ± 14.6	-	Xu et al. (2013)
Mt. Leigong	China	2178	26.39° N	108.2° E	Remote forest	05/2008-05/2009	2.80 ± 1.51	-	-	Fu et al. (2010)
Mt. Walinguan	China	3816	36.287°N	100.898°E	Remote grassland	09/2007-09/2008	1.98 ± 0.98	19.4 ± 18.0	7.4 ± 4.8	Fu et al. (2012a)
Nanjing	China	100	32.05° N	118.78° E	Urban	01-12/2011	7.90 ± 7.00	-	-	Zhu et al. (2012)
						06/2011-02/2012		1100 ± 570*	-	Zhu et al. (2014)
Ningbo	China	10	29.867° N	121.544° E	Urban	10/2007-01/2008	3.79 ± 1.29	-	-	Nguyen et al. (2011)
Qingdao	China	40	36.16° N	120.5° E	Urban	01/2013	2.80 ± 0.90	245 ± 174*	-	Zhang er al. (2014)
Seul	Korea	17	37.514° N	127.001° E	Urban	02/2005-02/2006	3.22 ± 2.10	23.9 ± 19.6	27.2 ± 19.3	Kim et al. (2009)
Shangai	China	19	31.23° N	121.54° E	Urban	08-09/2009	2.70 ± 1.70	-	-	Friedli et al. (2011)
						07/2004-04/2006	-	560 ± 220*	-	Xiu et al. (2009)
Shangri-La	China	3580	28.017° N	99.733° E	Remote forest	11/2009-10/2010	2.55 ± 2.73	37.8 ± 31.0	7.9 ± 7.9	Zhang er al. (2015)
Southeastern coastal cities	China	-	-	-	Urban	11/2010, 01&04&08/2011	-	141 ± 128	-	Xu et al. (2013)
Tokai-mura	Japan	15	36.27°N	140.36°E	Urban	10/2005-08/2006	3.78 ± 1.62	-	-	Osawa et al. (2007)
Wanqingsha	China	3	22.7° N	113.55° E	Remote coast	11/12/2009	2.94	-	-	Li et al. (2011)
Wuhan	China	20	30.6° N	114.3° E	Urban	-/2002	14.8		-	Xiang and Liu (2008)
Xiamen	China	7	24.60° N	118.05° E	Urban	03/2012-02/2013	3.50 ± 1.61	174 ± 280	61 ± 69	Xu et al. (2015)

*(PBM/TPM: * Indicates TPM (total particulate-bound mercury) and the rest indicate PBM (particulate-bound mercury on particles with an aerodynamic diameter < 2.5 μm)*

6378
6379

Table 9: Hg concentrations and deposition fluxes in precipitation, throughfall, and litterfall in China (from Fu et al., 2015).

Site	Elev (m asl)	Lat	Lon	Type	Study period	Samples	Hg concentration (ng L^{-1} or ng g^{-1})		Deposition flux ($\mu g\ m^{-2}\ yr^{-1}$)		Reference
							THg	MeHg	THg	MeHg	
Mt. Ailao, Yunnan	2500	24,53	101,02	Remote	06/2011-05/2012	Precipitation	3,0	-	5,4	-	Zhou et al. (2013)
						Litterfall	54,0		71,2	-	
Mt. Leigong, Guizhou	2178	26,39	108,20	Remote	05/2008-05/2009	Precipitation	4,0	0,04	6,1	0,06	Fu et al. (2010b)
						Throughfall	8,9	0,1	10,5	0,12	
						Litterfall	91,0	0,48	39,5	0,28	
Mt. Damei, Zhejiang	550	29,63	121,57	Remote	08/2012-07/2013	Precipitation	4,4	-	7,0	-	Lang (2014)
						Litterfall	46,6	-	26,0	-	
Nam Co, Tibet	4730	30,77	90,99	Remote	07/2009-07/2011	Precipitation	4,8	0,03	1,8	0,01	Huang et al. (2012)
Mt. Gongga[1], Suchuan	1640	29,65	102,12	Remote	12/01/06	Precipitation*	9,9	-	9,1	-	Fu et al. (2008)
Mt. Gongga[2], Suchuan	3000	29,58	101,93	Remote	05/2005-04/2007	Precipitation*	14,2	0,16	26,1	0,3	Fu et al. (2010a)
						Throughfall	40,2	0,3	57,1	0,43	
						Litterfall	35,7	-	35,5	-	
Mt. Changbai, Jilin	750	42,40	128,47	Remote	08/2005-07/2006	Precipitation*	13,4	-	8,4	-	Wan et al. (2000a)
Puding, Guizhou	1145	26,37	105,80	Remote	08/2005-07/2006	Precipitation*	20,6	0,18	24,8	0,22	Guo et al. (2008)
Hongjiadu, Guizhou	1130	26,88	105,85	Remote	08/2005-07/2006	Precipitation*	39,4	0,18	34,7	0,16	Guo et al. (2008)
Yinzidu, Guizhou	1088	26,57	106,12	Remote	08/2005-07/2006	Precipitation*	35,7	0,18	38,1	0,19	Guo et al. (2008)
Dongfeng, Guizhou	970	26,85	106,13	Remote	08/2005-07/2006	Precipitation*	37,4	0,2	36,3	0,19	Guo et al. (2008)
Wujiangdu, Guizhou		27,32	106,77	Remote	08/2005-07/2006	Precipitation*	57,1	0,25	39,6	0,17	Guo et al. (2008)
Guiyang	1040	26,57	106,72	Urban	09/07/08	Precipitation	13,3	0,05	13,4	0,05	Liu et al. (2011)
Xiamen	50	24,60	118,31	Urban	07/2013-02/2014	Precipitation	26,6	-	30,4	-	Wu (2014)
Chongqing				Urban	06/2010-06/2011	Precipitation	30,7	0,31	28,7	0,28	Wang et al. (2012); Y.M. Wang et al. (2014)
Tieshanping, Chongqing	500	29,63	104,68	Urban	03/2005-03/2006	Precipitation	32,3	-	29,0	-	Wang er al. (2009)
						Throughfall	69,7	-	71,3	-	
						Litterfall	105	-	220	-	
Nanjing	100	32,05	118,78	Urban	06/2011-02/2012	Precipitation	52,9	-	56,5	-	Zhu et al. (2014)

*(Precipitation: * indicates bulk precipitation and the rest indicate wet-only precipitation. Mt. Gongga: [1] elevation of the sampling site was 1600m above sea level. [2] Elevation of the sampling site was 3000m above sea level).*

3.2.5 Mercury concentrations and pattern analysis in polar areas (Arctic and Antarctica)

Arctic ecosystems and indigenous communities are particularly vulnerable to methylmercury exposures due to its biomagnification in many traditionally consumed foods such as birds, fish and marine mammals. In order to reduce negative health effects associated with methylmercury exposures, the pathway from emissions to human and environmental impacts needs to be understood. Atmospheric modelling provides a first step by tracing the link from emissions to deposition onto environmental surfaces. Deposition of mercury in a particular region depends on the magnitude and speciation of domestic and foreign emissions and on the oxidative capacity of the atmosphere that transforms gaseous elemental mercury (GEM) to deposited divalent species (UNEP, 2015). Atmospheric deposition is partly offset by the re-emission of a fraction of deposited mercury. Atmospheric Hg deposition from different models compares fairly well (add reference). Further detailed information on modelling uncertainty and scenario analysis can be found in Chapter 4 of this GMA report.

Located far from anthropogenic emissions, Polar Regions can be seen as open-air laboratories to improve our understanding of these atmospheric processes.

The Arctic Monitoring and Assessment Programme (AMAP) established in 1991, is a coordinated air monitoring programme covering the circum-Arctic areas of North America and Eurasia. The AMAP programme has an active ambient air Hg monitoring component with sites in Canada, USA, Russia, Norway and Greenland (Denmark). The Global Atmospheric Watch (GAW) site at Alert operated by Environment and Climate Change Canada – and funded through the Northern Contaminants Program (NCP) of Indigenous and Northern Affairs Canada (INAC) – has the longest continuous record of GEM (22 years) and Hg speciation (15 years) in the Arctic (Cole et al., 2013; Steffen et al., 2014). Continuous monitoring for long periods has also occurred at: (1) Amderma (Russia) (Steffen et al., 2005), (2) GAW Ny-Ålesund 'Zeppelin' site (Svalbard, Norway) (Berg et al., 2013), (3) AMAP Villum Research Station at Station Nord (hereafter named Station Nord, Greenland-Denmark) (Skov et al., 2004), and (4) Andøya (northern Norway) (Berg et al., 2001). Four multi-year records over the 2011-2015 period from high arctic (Alert, Station Nord and Zeppelin) and European sub-arctic (Andøya) sites were recently analysed (Angot et al., 2016a). Additionally, summertime measurements were performed in 2004 over the North Atlantic Ocean (Aspmo et al., 2004), and in 2005, 2010 and 2012 in the marine boundary layer over the Arctic Ocean (Sommar et al., 2010, Yu et al., 2014).

		ALT	SND	NYA	AND	TR	DC	DDU
2011	*n*	8040	4712	8173	7444	5978	NA	NA
	mean	1.39	1.26	1.51	1.61	0.95	NA	NA
	median	1.35	1.34	1.59	1.61	0.99	NA	NA
	SD	0.45	0.32	1.61	0.15	0.20	NA	NA
2012	*n*	8447	7932	8181	8428	7808	3761	5949
	mean	1.21	1.44	1.51	1.61	0.98	0.76	0.91
	median	1.21	1.44	1.54	1.61	0.97	0.70	0.92
	SD	0.35	0.26	0.21	0.13	0.15	0.24	0.20
2013	*n*	8048	6605	6980	7862	8197	2900	5121
	mean	1.31	1.57	1.47	1.53	0.90	0.84	0.85
	median	1.39	1.49	1.52	1.56	0.93	0.87	0.85
	SD	0.46	0.44	0.30	0.15	0.15	0.27	0.19
2014	*n*	8358	4991	6730	8146	7421	NA	1958
	mean	1.45	1.36	1.48	1.50	0.95	NA	0.85
	median	1.45	1.36	1.57	1.51	1.00	NA	0.82
	SD	0.33	0.35	0.33	0.16	0.21	NA	0.38
2015	*n*	NA	1059	8342	7146	3670	8383	3114
	mean	NA	1.11	1.49	1.50	0.94	1.06	0.86
	median	NA	1.11	1.49	1.50	0.93	1.12	0.87
	SD	NA	0.32	0.21	0.10	0.31	0.41	0.19

Table 10: Annually based statistics (number of hourly-averaged data (n.), mean, median, standard deviation (SD), of Hg(0) concentrations (in ng m^{-3}) at ground-based polar sites over the 2011-2015 period.

While the Arctic has been extensively monitored, with hundreds of publications focusing on AMDEs, measurements are more sporadic in Antarctica. Several short-term ambient air measurements campaigns were carried out in summer in the 2000s at Terra Nova Bay, McMurdo, South Pole and Concordia stations (Sprovieri et al., 2002; Brooks et al., 2008a, b; Dommergue et al., 2012). A year-round record (January 2000-February 2001) was reported at Neumayer (Ebinghaus et al., 2002; Temme et al., 2003) while multi-year records of GEM were initiated at the Norwegian Antarctic Research Station, Troll (TR) in 2007 (Pfaffhuber et al., 2012). In 2012, GMOS (2011-2015) supported the implementation of two other monitoring stations: Dumont d'Urville on the East Antarctic coast and Concordia station on the East Antarctic ice sheet (Angot et al., 2016b, c). Monitoring at Concordia station is now supported by the French Polar Institute IPEV. Additionally, short-term field campaigns dedicated to atmospheric Hg (Nerentorp Mastromonaco et al., 2016; Wang et al., 2016) and Hg deposition (Han et al., 2011; 2014; 2017) were performed in recent years over the Austral Ocean and the East Antarctic ice sheet, producing supplementary data. In Nerentorp Mastromonaco et al., 2016, the authors suggested a seasonal increase of total mercury in the sea-water due to a contribution of Hg(II) deposition combined with contributions from melting sea ice and snow.

First discovered in 1995 (Schroeder et al., 1998), atmospheric mercury depletion events (AMDEs) are observed in springtime throughout the Arctic (Lindberg et al., 2001; Berg et al., 2003a; Poissant and Pilote, 2003; Skov et al., 2004; Steffen et al., 2005) as a result of the oxidation of GEM by reactive bromine species (Lu et al., 2001; Brooks et al., 2006; Sommar et al., 2007). AMDEs can lead to the deposition of ~100 t of mercury per year to the Arctic (Ariya et al., 2004; Skov et al., 2004; Dastoor et al., 2015). The fraction of mercury retained in snowpack during AMDEs is still a matter of debate in the scientific mercury community because a number of studies have observed rapid revolatilization (Steffen et al., 2008; Soerensen et al., 2016).

Several studies have reported significant re-emission (e.g., Ferrari et al., 2005; Brooks et al., 2006; Kirk et al., 2006; Sommar et al., 2007; Dommergue et al., 2010a) reducing the amount of mercury that accumulates within the snowpack (Hirdman et al., 2009; Larose et al., 2010). Until today no one has determined a net accumulation based on flux measurements of wet deposition, dry deposition and reemission. During AMDEs, dramatically higher levels of both gaseous oxidised mercury (GOM; formerly named reactive gaseous mercury, RGM) and/or $PBM_{2.5}$ are observed (Lu et al., 2001; Lindberg et al., 2002; Lu and Schroeder, 2004; Sprovieri et al., 2005; Steffen et al., 2008). Lindberg et al. (2002) for instance reported GOM concentrations up to 900 pg m^{-3} during an AMDE at Barrow (Alaska) and

showed a strong positive correlation between GOM production and both UV-B radiation and surface snow Hg concentrations. Preliminary multi-year trends of GOM and $PBM_{2.5}$ concentrations at Alert were analysed (Cole et al., 2013), indicating increases from 2002 to 2009 in both GOM and $PBM_{2.5}$ during spring when concentrations are highest. Steffen et al. (2014) investigated the behaviour of the GOM and $PBM_{2.5}$ over 10 years at Alert and showed that there is a transition to a regime of high $PBM_{2.5}$ levels in March and April to a regime of high GOM levels in May. This transition was found to be driven by air temperature and presence of springtime particles (sea salts and arctic haze). They further reported that the highest deposition of mercury to the snow occurs when the GOM levels peak and not when $PBM_{2.5}$ levels are highest. They concluded that, using this information, one can predict when the most mercury will be deposited to the snow and ice surfaces in the high Arctic. Despite the significant challenges in the measurements, the behaviour of mercury over the Arctic sea ice has been investigated (Nghiem et al., 2012; Steffen et al., 2013; Moore et al, 2014). Nghiem et al (2012) showed that the ever decreasing amount of perennial sea ice in the Arctic Ocean will impact the amount of active bromine in this area. Since the depletion of GEM is driven by the bromine photochemistry, the decrease in perennial sea ice will certainly impact the amount of mercury depleted in the atmosphere over the Arctic sea ice. Further, Moore et al. (2014) showed that with the changes of sea ice from perennial to annual, the dynamics of the sea ice also change. Annual sea ice creates more dynamic sea ice, enabling it to provide more turbulence within the ice and produce more open leads. These open leads cause convective forcing of the overlying atmosphere to pull down air masses that contain more mercury than those which are depleted at the surface and replenish the pool of mercury available for conversion and eventual deposition. Finally, it has also been shown that some of the mercury deposited to the surfaces is reemitted to the atmosphere (references above); however, several studies have shown that photo-reduction of the mercury in the snow is dependent on the amount of chlorine in the surface snow (Poulain et al., 2004 and Lehnherr and St Louis, 2009). Thus, the more chlorine in the snow, the less mercury will reemit. Steffen et al. (2013) demonstrated that there is significantly more GEM re-emitted to the atmosphere from inland snow that from snow over the sea ice. All of these studies combined demonstrate that the mercury chemistry in the Arctic is very dependent on the sea ice and its overlying atmosphere. With significant changes occurring in the Arctic and the dynamics of the sea ice, the springtime mercury cycle will be impacted including the amount of mercury deposited and retained in the Arctic ecosystem.

As presented in Fig. 4, a different seasonal pattern is observed in the high Arctic (ALT, SND, NYA – latitude ranging from 78 to 82°N) as compared to lower latitudes (AND, northern Norway - 69°N). As noted by Angot et al. (2016a), a variability is observed at high Arctic sites in spring due to the occurrence of AMDEs (see above). Summertime (June-August) measurements also differ from what is seen at lower latitudes likely due to re-emission of GEM by the Arctic Ocean and/or by snow surfaces (Angot et al. 2016a and references therein). Yu et al. (2014) reported highly variable GEM concentrations (0.15-4.58 ng m^{-3}) over the central Arctic Ocean in summer, highlighting the need for additional oceanographic campaigns to better understand and constrain oceanic fluxes of GEM.

The analysis of ten-year trends of TGM (GEM+GOM) concentrations (Cole et al., 2013) revealed discrepancies among Arctic sites. While no trend was observed at Zeppelin station, a slight decreasing trend (-0.9% per year) was reported at Alert. This difference in trends may be due to several factors including different air masses origin and local scale processes (e.g., oceanic evasion).

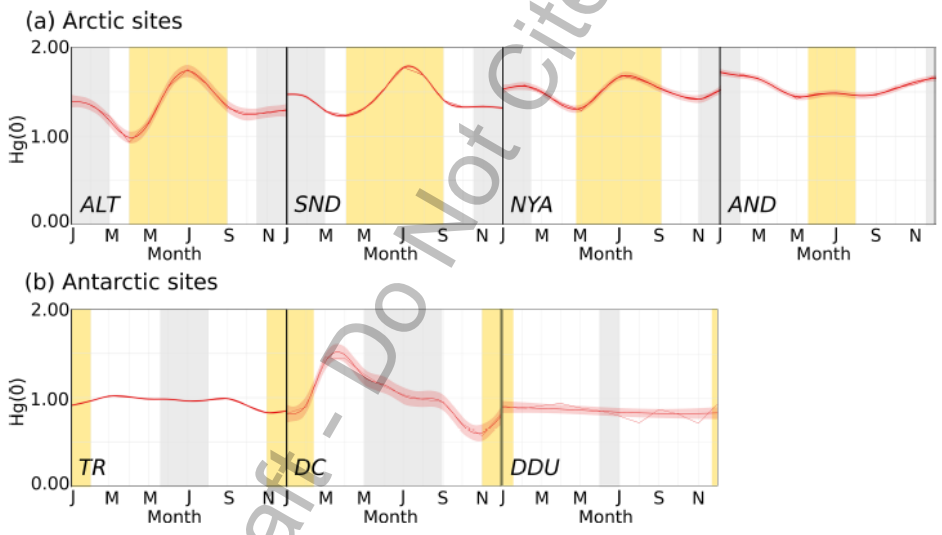

Figure 4: Seasonal variation (monthly mean along with the 95% confidence interval for the mean) of GEM (Hg(0)) concentrations (in ngm^{-3}) at (a) four Arctic and (b) three Antarctic sites for the period 2011-2015 (Angot et al., 2016a). ALT: Alert, SND: Villum Research Station at Station Nord, NYA: Zeppelin station at Ny-Ålesund, AND: Andøya, TR: Troll, DC: Concordia Station at Dome C, DDU: Dumont d'Urville. Periods highlighted in yellow (grey) refer to 24h sunlight (darkness).

Similar to the Arctic, AMDEs can be observed at coastal Antarctic sites after polar sunrise (e.g., Ebinghaus et al., 2002). However, major differences between the Artic and the Antarctic Hg atmospheric cycles have been identified in recent studies, primarily because of their different geography; While the Arctic is a semi-enclosed ocean almost completely surrounded by land, Antarctica is a land mass –

covered with an immense ice shelf – surrounded by ocean. In summer (November to mid-February, permanent sunlight), GEM concentrations exhibit a distinct diurnal cycle on the East Antarctic ice sheet, with a maximum at noon, attributed to a dynamic daily cycle of GEM oxidation, deposition to the snowpack, and re-emission from the snowpack (Dommergue et al., 2012, Angot et al., 2016c, Wang et al., 2016). Additionally, GEM depletion events can be observed on the ice sheet in summer, with GEM concentrations remaining low (~ 0.40 ng m^{-3}) for several weeks (Angot et al., 2016c). These depletion events do not resemble the ones observed in springtime in the Arctic since they are not associated with depletion of ozone. They are observed when air masses stagnate over the East Antarctic ice sheet, likely favouring an accumulation of oxidants within the shallow (few hundreds of meters) atmospheric boundary layer. These observations, along with GOM/ $PBM_{2.5}$ concentrations up to 1 000 pg m^{-3} recorded at South Pole (Brooks et al., 2008), suggest that the inland atmospheric reservoir is depleted in GEM and enriched in GOM in summer. Observations at coastal Antarctic stations suggest that divalent Hg species produced inland can be transported – due to the large-scale airflow pattern flowing from the East Antarctic ice sheet towards the coast (katabatic winds) – leading to Hg deposition and accumulation in coastal ecosystems (Angot et al., 2016b, Bargagli, 2016). Atmospheric models are currently unable to reproduce this complex reactivity (Angot et al., 2016a). Field studies also show that the sea ice environment is a significant interphase between the polar ocean and the atmosphere and should be accounted for when studying how climate change may affect the mercury cycle in polar regions (Nerentorp Mastromonaco et al., 2016b).

3.2.6 Atmospheric mercury measurements and trends in Europe

Heavy metals were considered by the Convention on Long-Range Transboundary Air Pollution (CLRTAP) beginning in the 1980s. At that time, mercury was only of secondary priority, as it was considered that measurements of the relevant chemical forms, and the understanding of chemistry involved, was not mature enough for any regional scale harmonized monitoring to be initiated (EMEP-CCC, 1985). The European Monitoring and Evaluation Programmes (EMEP) first data report on heavy metals (EMEP, 1986) does thus not include any Hg data, even though first measurements were already available at that time. By 1990, the number of sites measuring mercury in air had increased to seven, with sites located in Norway, Sweden, Denmark, Germany and the UK. Mercury was included in the first priority list of measurements for the late 1990s, and since then the number of sites have increased gradually. The CLRTAP Aarhus Protocol on Heavy metals was adopted in 1998, and countries agreed to reduce their

6536 emission rates compared to year 1990 levels. Currently monitoring efforts include about 37 sites across
6537 17 countries (Fig. 5). Considering all years, the total number of sites is 64 sites and 23 countries.

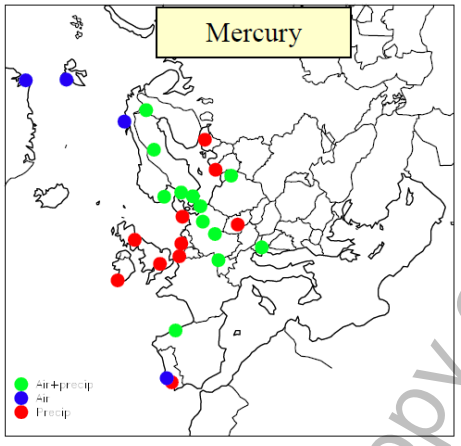

6538
6539 **Figure 5:** EMEP Mercury observation network.
6540

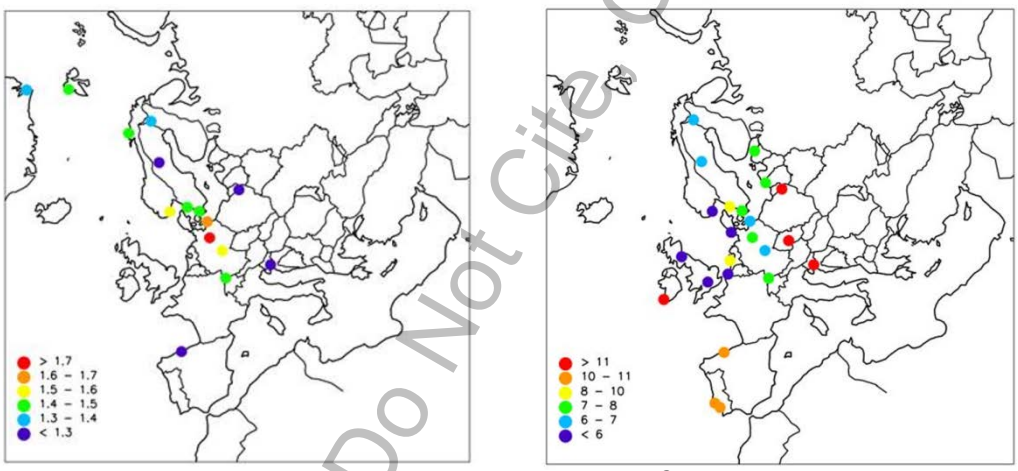

6541
6542 **Figure 6:** Concentration levels of Mercury in air (left, unit: ng/m^3) and precipitation (right, unit ng/L) at
6543 EMEP sites, year 2014.

6544 Compared to other heavy metals, relatively few stations are measuring mercury in precipitation in
6545 Europe, and many of them are related to the OSPARCOM programme. There are several sites (in PT, LV,
6546 IE) with high detection limits and these are only giving an indication of upper concentration limit. There
6547 is no clear regional distribution of mercury in precipitation; the highest concentration is seen at NL0091
6548 with 10 µg/L (when excluding uncertain data from Portugal and Ireland), followed by sites in Czech
6549 Republic and Sweden with concentrations of 8 µg/L, while the lowest levels (less than 5 µg/L) are seen in
6550 Great Britain (7).

6551 Annual averages of Hg concentrations in precipitation and in air in 2014 are presented in Figure 6. There
6552 is indication of elevated level in central Europe as expected due to influence from anthropogenic

sources like coal combustion. An interesting observation is that the coastal Arctic sites in Norway has slightly higher levels than what is observed at Greenland and more inland in Finland and Sweden, which might be due to the summertime evasion from the ocean or due to the fact that Svalbard receives several direct transport episodes from the continent, especially in winter and spring. PL05 and SI08 show unexpected low concentration, 1.2 ng m^{-3} and 0.8 ng m^{-3} respectively. The latter concentration level is even lower than observed in Antarctica (Pfaffhuber et al, 2012). Given the locations of these stations and the proximity to emission sources, it seems like there may be a bias in the concentration level for these two sites. This bias is larger at ES08, which has an annual mean of 0.3 ng m^{-3}, which obviously cannot be correct.

Results from a field intercomparison study of mercury measurement within EMEP performed in 2005 showed that most participating labs performed well and within the +-30% uncertainty EMEP data quality objective (Umweltbundesamt, 2006, Weigelt et al., 2013). However, the biased concentration results reported above highlights the importance to follow QA/QC procedures. These three laboratories need to evaluate their methodology as it seems evident that there is an issue with either calibration or gold trap poisoning, or a combination of both. In precipitation, the highest levels are seen in Eastern Europe (SI, PL and CZ), which seem reasonable since the anthrophonic emission sources are highest in this region. Taking into account that precipitation measurements of mercury are more complex than air measurements, and that the expected measurement uncertainty is 42% (Umweltbundesamt, 2006), the observed concentrations and spatial pattern seems reasonable, for Poland most of the data is below detection limit so it is difficult to fully assess the spatial concentration pattern. Also, Ireland and Portugal report most of the data below detection limit.

Two recent publications and reports present the spatial and temporal trends of mercury in EMEP, namely Tørseth et al. (2012) and Colette et al. (2016). The first paper study provides a very broad introductory overview of the full dataset available, but does not go into any details on site level and individual time series. The latter report focuses primarily on the period 1990-2012, and relies heavily on model results from the EMEP-MSC-E model, using official emissions data. An overall assessment based on these two publications is given below.

Figure 7 presents annual time series of mercury measured at sites with long-term data series across Europe. As can be seen, most of these sites are located in Northern Europe, and there are obvious gaps in the time series in the early 1990s. Inter-annual variability is large, but a significant reduction has

6583 occurred since. Trends based on this analysis suggest reductions in the order of 5-10% since the late
6584 1990s. More recent work by Zhang et al. (2016) suggests declines of greater than 2% per year since the
6585 mid-1990s in Western Europe and a total reduction of greater than 30% due to declines in primary
6586 anthropogenic source releases.

6587

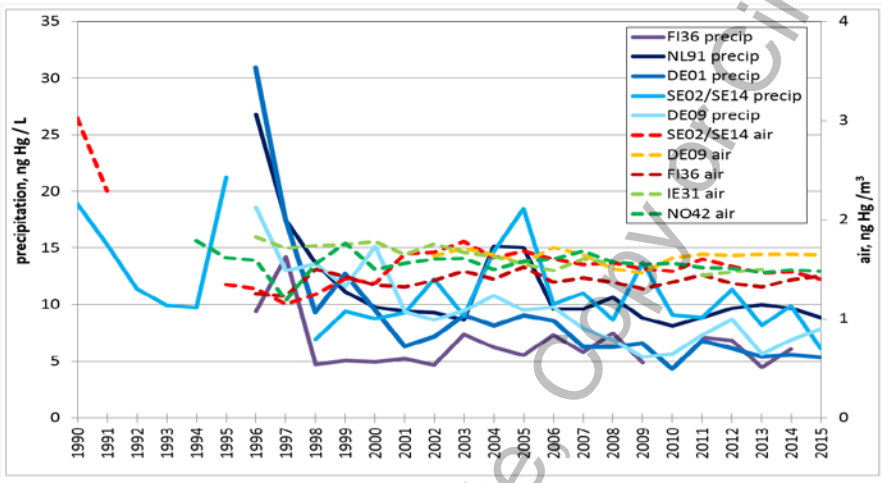

6588
6589
6590 **Figure 7:** Time series of mercury in air and precipitation at selected EMEP stations, 1990-2015.
6591

6592 Tørseth el al., 2012 also include reference to various studies on trends in emissions and observations, to
6593 assess the levels before the late 1980ies. They conclude that a major decline of the European Hg
6594 emissions occurred at the end of the 1980s. The measurements of total gaseous mercury (TGM) for the
6595 period from 1980 to about 1993 indicate a dramatic decrease of about 60% in ambient concentrations.
6596 Concentration changes reflect the emission change in Europe. Reduced emissions in Europe and the long
6597 lifetime of Hg have resulted in an increased focus on non-European sources (HTAP, 2010).
6598 Measurements of total gaseous mercury indicate e.g. a dramatic decrease in concentrations during 1980
6599 to about 1993.

6600 For mercury, the European sources have been reduced significantly resulting in a relatively large
6601 contribution from non-European sources to ambient levels. The monitoring efforts within Europe have
6602 gradually improved in Northern Europe, while other regions have little data.

6603 ### 3.2.7 Northern–Southern Hemispheric gradients

6604 A summary of descriptive statistics of GEM, GOM and PBM from all GMOS sites in the Northern and
6605 Southern Hemispheres as well as in the Tropical area is reported in Tables 2 and 3, whereas Figure 8

shows a focus on GEM yearly distribution for 2013 (blue) and 2014 (green). The sites have been organized in the graphic as well as in the tables according to their latitude from those in the Northern Hemisphere to those in the tropics and in the Southern Hemisphere. The box-and-whisker plot of GEM shows a downward trend with the 13 northern sites which had significantly higher median concentrations than the southern sites did, confirming the assessment made on long-term monitoring sites such as Mace Head (MHD), Ireland (Ebinghaus et al., 2011; Weigelt et al., 2015), and at Cape Point (CPT), South Africa (Slemr et al., 2015). At MHD the annual baseline GEM means observed by Ebinghaus et al. (2011) decreased from 1.82 ngm^{-3} earlier in 1996 to 1.4 ngm^{-3} in 2011, showing a downwards trend of 1.4–1.8% per year. Recently across the GMOS network, a decrease of 1.6% at MHD from 2013 and 2014 was observed and a slight increase in Hg concentrations at CPT from 2007 to 2013 that continued through 2014 (Slemr et al., 2015). The clear north–south gradient, in line also with previous studies (Soerensen et al., 2010a, b, 2012; Sommar et al., 2010; Lindberg et al., 2007; Sprovieri et al., 2010), has in addition confirmed by the probability density functions (PDFs) of the data (Sprovieri et al., 2016).

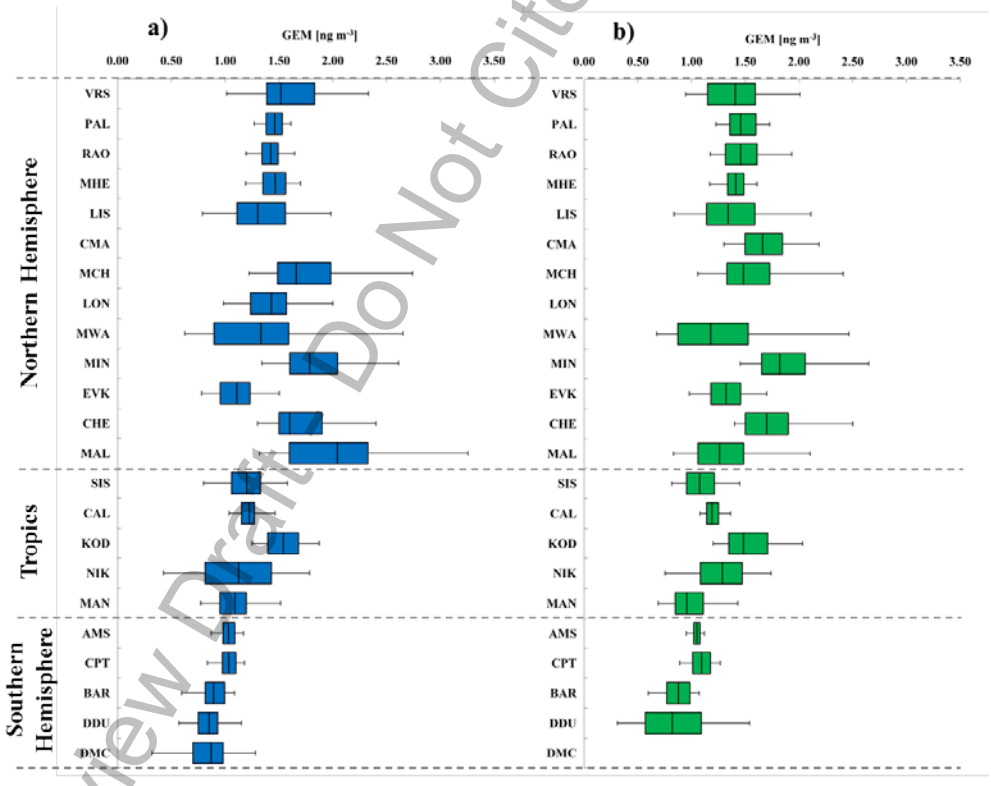

Figure 8: Box-and-whisker plots of GEM yearly distribution at the GMOS stations for (a) 2013 and(b) 2014. The sites are organized according to their latitude from the northern to the southern locations. Each box includes median(midline), 25th and 75th percentiles (box edges), 5th and 95th percentiles (whiskers) (Sprovieri et al. 2016).

3.3 Vertical profile and UTLS measurements

3.3.1 Vertical profiles

Vertical profiling of GEM from inside the boundary layer to the free troposphere was carried out during European Tropospheric Mercury Experiment (ETMEP) flights in 2013 (Weigelt et al. 2015). Several flights were performed with a CASA-212 research aircraft equipped with scientific instruments to measure GEM, GOM, and TGM as well as the trace gases CO, O_3, SO_2, NO, NO_2, and meteorological parameters temperature, pressure, and relative humidity. A specially designed gas inlet system was installed at the aircraft fuselage. In total five vertical profiles were flown over flat and mountainous rural- and industrialized sites in Slovenia and Germany. On the contrary to previously measured vertical profiles, a significant difference between boundary layer- and free tropospheric air was detected. While the free tropospheric overall GEM background concentration over central Europe is ~ 1.3 ng m^{-3} inside the boundary layer the GEM background concentration was found to be 10 to 30% higher (~ 1.6 ng m^{-3}). At all measurement locations, neither in the boundary layer, nor in the free troposphere a clear vertical gradient was apparent. This finding indicates that inside the particular layers of the atmosphere, GEM is homogeneously distributed. The combination of ETMEP measurements over Leipzig with CARIBIC measurement over Western Europe (Fig. 9) revealed for the first time a complete vertical profile from 0.5 km (lower boundary layer) to 10.5 km (upper free troposphere). From above the boundary layer to the free troposphere's top the GEM background concentration is on average 1.3 ng m^{-3}. All concentrations are given at STP (0°C, 1013.25 hPa).

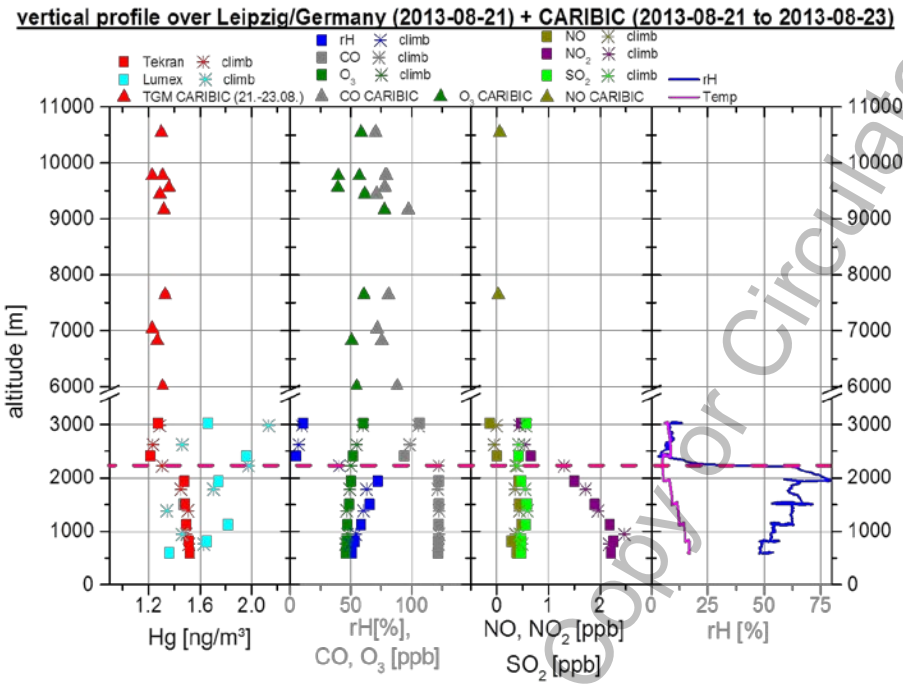

Figure 9: Vertical profile of GEM, CO, O3, SO2, NO, NO2, T, RH over Leipzig, Germany during ETMEP and CARIBIC flights.

3.3.2 Aircraft-based emission estimates for point and area sources

On several Nitrogen, Oxidants, Mercury and Aerosol Distributions, Sources and Sinks (NOMADSS) project flights large Hg point sources were sampled, mainly coal-fired power plants (CFPP) in the Southeast U.S. Ambrose et al. (2015), developed a unique method to use the NOMADSS data to evaluate Hg point source emissions. This method relies on the simultaneous C-130 observations of NO_x, SO_2, CO and CO_2 observations. A key conclusion is that for some CFPPs, including some of the largest Hg emitters in the US, the observations suggest substantially higher Hg emissions compared to the emission inventories.

During ETMEP flights over central Europe significant mercury emissions were measured from a modern coal fired power plant south of Leipzig/Germany. Inside the plume GEM peaked to 10 ng/m³. The denuder sample inside the plume indicated, modern coal-fired power plants may be an overestimated source of GOM. The measured fraction of GOM inside the plume was between 0.5% and 2%. This is in contrast to the 40%, given by the "AMAP/UNEP geospatially distributed mercury emissions dataset 2010v1" (AMAP/UNEP, 2013). The yearly emission of gaseous mercury from that power plant was estimated to 268-283kg/a for GEM and 2-12 kg/a for GOM. (Weigelt et al. 2015).

The Chicago-Gary area is highly industrialized with significant emissions of Hg and other pollutants. Using data from NOMADSS flight RF-15, Gratz et al. (2016) developed a novel method to evaluate the Hg

emission inventory from this region. The observations showed a region of enhanced Hg, CO, SO2 and NOx. Combining the observations with the Flexpart model allowed for the characterization of the "footprint" of the observations and therefore a good comparison between the observations and expectations based on the emission inventory. Gratz' analysis indicated "that there are many small emission sources that are not fully accounted for within the inventory, and/or that the re-emission of legacy Hg is a significant source of THg to the atmosphere in this region (Gratz et al., 2016).

3.3.3 Large-scale Tropospheric distribution and plumes

During the Civil Aircraft for the Regular Investigation of the atmosphere Based on an Instrument Container (CARIBIC) project more than 100 large-scale pollution plumes have been detected in the global upper troposphere. The largest plume with an extension of 1000 km was detected on a flight from Frankfurt to Osaka between the Korean peninsula and the Yellow Sea. This mixed plume could be attributed to large forest fires in Southern Siberia as well as industrial sources in Chinese provinces of Shandong, Henan, Shanxi and Hebei.

Most of the plumes were found over East Asia during the flights from Frankfurt to Guangzhou, Osaka, Seoul and Manila, in the African equatorial region during the flights to South Africa, over South America during the flights to Sao Paulo and Santiago de Chile, and over Pakistan and India during the flights to Chennai. The plumes encountered over the African equatorial region and over South America originate from biomass burning as evidenced by low Hg/CO emission ratios and elevated mixing ratios of acetonitrile, CH_3Cl and CH_3Br. Backward trajectories point to the region around Rift Valley and Amazon basin with its outskirts as the source areas. The plumes encountered over the East Asia and over Pakistan and India are predominantly of urban/industrial origin, sometimes mixed with products of biomass/biofuel burning. Numerous plumes with elevated mercury concentrations were encountered during the tropospheric sections of the CARIBIC flights since May 2005. Mercury correlated significantly with CO in more than 50% of the observed plumes and with CO_2 in about 30% of the plumes for which CO_2 data were available. Extensive ancillary data on chemical fingerprint of the air within these plumes and backward trajectories provide additional means to identify the origin and the type of the source (Slemr et al., 2014).

Large plumes over equatorial Africa were observed during all flights between Frankfurt and South Africa. These plumes which extend over thousands of km are embedded in north-south gradient of mercury, CO, and CO_2, and consist of a number of overlapping smaller plumes. Due to the changing background,

the inhomogeneity of the plumes and low precision of the mercury measurements only a few of the plume encounters provided significant Hg vs. CO correlations. Most plumes were observed over Far East Asia and relative to the number of flights to Far East destinations the yield of plumes with significant Hg vs CO correlations was the second highest after the African flights. Lower yields of plume occurrence were found for flights to South America and to South Asia. Only one plume was encountered over North America and one over Europe. (Slemr et al., 2009, Slemr et al., 2013, Slemr et al., 2014)

The Hg/CO emission ratios derived from these correlations are consistent with the previous data and tend to smaller values of ~1 pg m^{-3} ppb^{-1} for plumes from biomass burning and larger values of ~6 pg m^{-3} ppb^{-1} for urban/industrial emissions. Most of the plumes observed over South America and Africa originate from biomass burning and one plume observed over mid-Atlantic could be attributed to forest fires in south eastern US. The plumes observed over the Far East Asia are mostly of urban/industrial or mixed origin. Only a few Hg/CO_2 emission ratios have been reported so far. The range of the Hg/CO_2 emission ratios from CARIBIC flights is comparable to the range observed at Cape Point (Brunke et al., 2012). The Hg/CO_2 emission ratios of 107 – 964 pg m^{-3} ppm^{-1} observed in the plumes over Far East, however, are substantially higher than 2 – 30 pg m^{-3} ppm^{-1} calculated by Brunke et al. (2012) for coal burning. If confirmed by further measurements the higher observed than calculated Hg/CO_2 emission ratios would imply substantial other mercury emissions than from coal burning. Generally it can be concluded from CARIBIC data that the major industrial sources for atmospheric mercury are located in East-Asia, Pakistan and India whereas major contribution to mercury emissions from biomass burning are originating from Equatorial Africa (Rift-Valley) and the Amazon region.

In the tropospheric CARIBIC data an El Niño Southern Oscillation (ENSO) signal could be detected. (Slemr et al., 2016a). The highest mercury concentrations are always found at the most negative SOI values i.e. are related to the El Niño events. A cross-correlation reveals that peak mercury concentrations are delayed by 6 – 12 months against SOI. This delay is similar to the delay of CO which has been shown to originate from biomass burning in aftermath of El Niño events. Slemr et al. (2016) suggested that the ENSO signal in the worldwide mercury concentrations is also due to mercury emissions from biomass burning (Slemr et al., 2009, Slemr et al., 2013, Slemr et al., 2014).

3.3.4 Airborne observations of speciated Hg

Mercury observations on the NCAR C-130 were made by the University of Washington in summer 2013 with specially developed Detector for Oxidized Hg Species (DOHGS) (Ambrose et al., 2015), which

measures both gaseous elemental mercury (Hg0), gaseous oxidized mercury (GOM), plus a fraction of particle-bound oxidized Hg. GOM is believed to consist of Hg(II) compounds, such as $HgCl_2$, $HgBr_2$, etc. The measurements were routinely calibrated in-flight with a high precision source of Hg0, and in the laboratory with sources of gaseous $HgBr_2$ and $HgCl_2$. The dual channel difference method avoids problems with earlier measurements based on KCl denuders, which are known to have significant interferences. We believe these are the most carefully calibrated and accurate measurements of speciated Hg made to date on an aircraft platform. Details on the methodology and further information on calibrations, accuracy, and precision are given in Ambrose et al. (2015). On several flights, substantial concentrations of Hg(II) were identified. Although the location and timing of these events were correct in the GEOS-Chem Hg model, the concentrations were much higher (2–4x). Figure 10 shows an example from research flight 6 (RF-06), along with the base simulations from GEOS-Chem (Gratz et al., 2015). This flight was also one of the few with detectable concentrations of BrO. We concluded that the likely source of Hg(II) on this flight was oxidation of gaseous elemental mercury (GEM) by Br radicals. This was supported by a detailed chemical mechanism and box-model calculation. This is a major finding and has implications for both Hg and halogens. Note that the halogen chemistry and mercury oxidation mechanism in the GEOS-Chem model were recently updated, as reported in Horowitz et al. (2017).

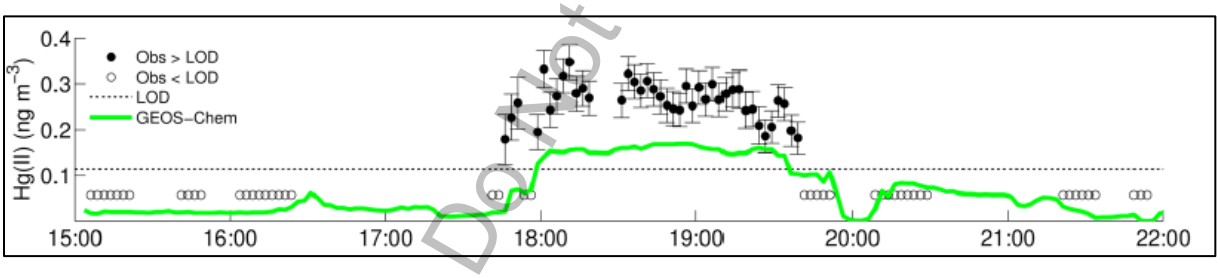

Figure 10: Oxidized Hg (Hg(II); ng m^{-3}) concentrations measured during RF-06 on June 19, 2013, (black points) and modelled Hg(II) from the base model simulations (green line).

Shah et al. (2016) further analysed the origins of oxidized mercury using a variety of sensitivity studies with the GEOS-Chem model. For observations above the detection limit it was found that modelled Hg(II) concentrations are a factor of 3 too low (observations: 212 ± 112 ng m^{-3}, model: 67 ± 44 ng m^{-3}). The highest Hg(II) concentrations, 300–680 pg m^{-3}, were observed in dry (RH < 35 %) and clean air masses during two flights over Texas at 5–7 km altitude and off the North Carolina coast at 1–3 km. The GEOS-Chem model, back trajectories and observed chemical tracers for these air masses indicate subsidence and transport from the upper and middle troposphere of the subtropical anticyclones, where fast oxidation of elemental mercury (Hg0) to Hg(II) and lack of Hg(II) removal lead to efficient

accumulation of Hg(II). Shah et al. (2016) suggested that the most likely explanation for the model bias is a systematic underestimate of the Hg0 +Br reaction rate, which has now been updated in Horowitz et al. (2017). It was shown that sensitivity simulations with tripled bromine radical concentrations or a faster oxidation rate constant for Hg0 +Br, result in 1.5–2 times higher modelled Hg(II) concentrations and improved agreement with the observations. The modelled tropospheric lifetime of Hg0 against oxidation to Hg(II) decreases from 5 months in the base simulation to 2.8–1.2 months in our sensitivity simulations. In order to maintain the modelled global burden of THg, we need to increase the in-cloud reduction of Hg(II) was increased, thus leading to faster chemical cycling between Hg0 and Hg(II). Observations and model results for the NOMADSS campaign suggest that the subtropical anticyclones are significant global sources of Hg(II).

In the lower stratosphere, TGM concentrations always decrease with increasing PV and O_3. This behaviour is similar to all trace species with ground sources and stratospheric sinks such as CO and CH_4. Opposite to such species, mercury as an element can only be transformed to other mercury species such as GOM or particle bound mercury (TPM). The transformation rate of TGM to particle bound mercury can be calculated using SF_6 as a timer. SF_6 is a very long-lived tracer whose concentration increases by about 0.230 ppt yr-1. Correlations of TGM with SF_6 suggest a seasonally dependent TGM conversion rate of about 0.43 ng m-3 yr-1 resulting in a stratospheric TGM lifetime of about 2 yr. This lifetime is longer than several weeks claimed recently by Lyman and Jaffe (2012) but is closer to 1 yr estimated by Holmes et al. (2010) using the GEOS-Chem model with included bromine oxidation chemistry.

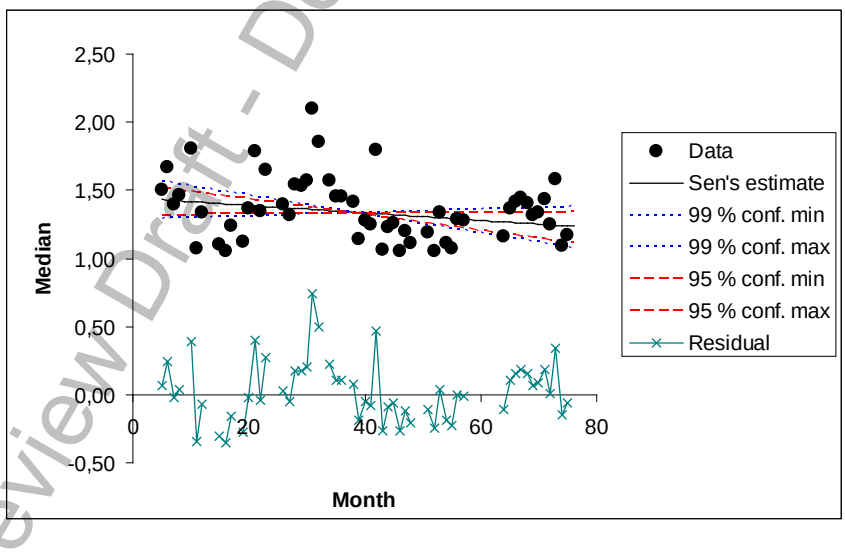

Figure 11: Monthly averages of TGM concentrations in the troposphere (PV < 1.5 PVU) north of 15°N from May 2005 to April 2011 with Sen´s slope estimate.

3.4 Temporal and spatial variability of Hg exchange fluxes between air and soil/vegetation/snow-ice

Re-emission of previously deposited Hg to terrestrial and aquatic surfaces is an essential component of the global biogeochemical Hg cycle, accounting for approximately 2/3 of inputs to the atmosphere each year (Amos et al., 2013; 2014). The magnitude of reemissions fluxes has grown substantially over the history of human use of mercury that has enriched terrestrial and aquatic ecosystems globally (Amos et al., 2013; 2015). Most evasion occurs as elemental Hg (Hg(0)) but in marine regions, dimethylmercury evasion ($(CH_3)_2Hg$) can also be important (Soerensen et al., 2016).

Globally, evasion of Hg(0) from the oceans in comparable in magnitude to primary anthropogenic emissions (Soerensen et al., 2010a). Concentrations of dissolved Hg(0) in seawater are driven by the supply of Hg(II) for reduction (total seawater Hg concentrations), biological and photochemical reduction rates mediated by light and bacterial activity, and the stability of Hg(II) complexes in seawater. Several recent studies have shown the composition of dissolved organic matter (DOM) in seawater can have a strong influence on the amount of Hg(II) that is reduced and subsequently evaded back to the atmosphere, with terrestrial DOM in particular effectively reducing reactivity of sorbed Hg (Soerensen et al., 2014; Schartup et al., 2015; Zhang et al., 2015). Net flux of mercury to the atmosphere through air-sea exchange is thought to range between 1940-4150 Mg per year, with a mean flux of 3200 predicted by Amos et al. (2013).

Air–soil (or vegetation covered) exchange fluxes are an important part of global and regional Hg biogeochemical cycle (Lindberg et al. 2007, Gustin et al. 2008, Gustin et al. 2010, Pierce et al. 2015). Much of Hg(II) deposited in precipitation or taken up plants is subject to reduction to Hg(0) and may be evaded back to the atmosphere. Smith-Downey et al. (2010) estimated based on a global terrestrial mercury model that evasion of mercury linked to decomposition of soil organic carbon pools and subsequent liberation of Hg(II) sorbed to soil organic matter is greater than 700 Mg per year, reflecting the large pool of Hg stored in terrestrial ecosystems globally (>240 Gg). In total, this study estimated 56% of Hg deposited to terrestrial ecosystems is reemitted. Similarly, Graydon et al. (2012) found that 45-70% of isotopically labelled Hg(II) wet deposited to a forested watershed had been reemitted to the atmosphere after one year. Recent observations suggest the evasion flux of mercury from global soils may be slightly lower and the reservoir even higher (e.g., Hararuk et al., 2013).

Hg exchange flux between soil (vegetation) depends on several environmental factors (soil moisture, soil porosity substrate temperature, etc.), chemical factors (Hg species and its content in soil, organic matter, atmospheric oxidants, etc.), meteorological factors (e.g. pressure, air temperature, wind speed and turbulence, solar radiation, snow cower) and surface characteristics (e.g. type of vegetation, substrate type, roughness of the surface) (Schroeder et al. 2005, Gustin et al. 2004). These factors are leading to highly variable Hg fluxes in different landscapes and determine spatial and temporal variability in deposition or evasion of GEM (Schroeder et al. 2005). All forms of atmospheric Hg can be deposited from atmosphere to soils or differently vegetated surfaces by wet or by dry deposition processes (Gustin 2011) where it can either remain in terrestrial system and undergo further biogeochemical cycle or emitted back to atmosphere with relative importance of different controlling factors (Gustin 2011). Changes in direction of the flux were observed on several soil types covered by different types of vegetation (Gustin and Jaffe 2010, Poissant et al. 2005), and can happen quickly, within few hours (Bash and Miller 2008, Converse et al. 2010).

Soil types, moisture, and Hg content and speciation in soil are important factors influencing GEM flux between soil and air (Kocman and Horvat 2010, Lin et al. 2010). Soil porosity and disturbance promote Hg(II) reduction and GEM transport from soil (Fu et al. 2012, Bash and Miller 2007). Soils with small grain size, silt and clay with higher surface area showed higher GEM fluxes to air (Gustin et al. 2002). Rainfall and soil moisture promote GEM emission by order of magnitude (Lindberg et al. 1999). Irrigation of soil enhances Hg (II) reduction and added water replaces GEM binding sites and thus promotes GEM emission. Organic matter in soil was reported to be one of main factors affecting GEM emissions as organic matter forms stable complexes with Hg(II) and thus reduce GEM flux (Grigal 2003, Skyllberg et al. 2006, Yang et al. 2007). Microbial activity in soil and increasing soil pH may promote GEM flux by Hg(II) reduction (Fritshe et al. 2008, Choi and Holsen 2009, Yang et al. 2007). High ambient air GEM concentrations were reported to reduce GEM flux by reducing Hg(0) concentration gradient and thus deposition is dominated despite influence of other factors (Xin and Gustin 2007, Bash and Miller 2007, Wang et al. 2007, Zhu et al. 2016). Flux measured from background soils was between -51.7 to 97.8 with mean of 2.1 ng $m^{-2}h^{-1}$ (Zhu et al. 2016 and references therein).

Vegetation is changing environmental factors at ground surfaces by reducing solar radiation, temperature, wind velocity (Gustin et al. 2004), and serve as surface for Hg uptake (Zhu et al. 2016). Deforestation can increase GEM emissions due to higher flor irradiation and temperature (Zhu et al. 2016, Carpi et al. 2014, Mazur et al. 2014). Recent measurements showed that GEM exchange flux

6835 between plants and air is bidirectional and that growing plants acts as a net sink (Ericksen et al. 2003,
6836 Stamenković et al. 2008, Hartman et al. 2009, Zhu et al. 2016). Most fluxes measured in forest foliage
6837 and grasslands were between -9.6 and 37 (6.3), and -19 to 41 (5.5) ng $m^{-2}h^{-1}$, respectively (Zhu et al.
6838 2016 and references therein).

6839 Air-snow exchange fluxes were mostly investigated in polar regions. During AMDEs air GEM is oxidized
6840 and deposited in snow as GOM and PBM which can be rapidly volatilized back to atmosphere by
6841 photochemical reduction on snow or in melted snow (Dommergue et al. 2003, Fain et al. 2007, Kirk et al.
6842 2006). Photo-reduction was found to be predominant factor for re-emission from snow and was linearly
6843 correlated to UV intensity (Lalonde et al. 2002, Mann et al. 2015). Important factor controlling snow-air
6844 fluxes is temperature also by changing solid-liquid water ratio (Mann et al. 2015). Similar factors as in
6845 polar regions control snow-air Hg exchange in temperate regions (Maxwell et al. 2013). Measured fluxes
6846 from snowpack are within same range reported for vegetation cower and were between -10.8 to 40 ng
6847 $m^{-2}h^{-1}$ with mean of 5.7 ng $m^{-2}h^{-1}$ (Zhu et al. 2016 and references therein).

6848 Polar air-sea water exchange of elemental mercury was for the first time measured continuously in the
6849 remote seas of western Antarctica. The measurements were performed during winter and spring (2013)
6850 in the Weddell Sea and during summer (2010/2011) in the Bellingshausen, Amundsen and Ross Seas,
6851 and show spatial and seasonal variations. The average DGM concentration in surface water in open sea
6852 was highest during spring (12±7pgL-1) and lowest during summer (7±6.8pgL-1), resulting in a net evasion
6853 of mercury during spring (1.1±1.6ngm-2 h-1) and a net deposition during summer (-0.2±1.3ngm-2 h-1).
6854 In open sea, higher average concentrations of GEM (or TGM) and DGM were found close to the Drake
6855 Passage compared to in the Bellingshausen and Weddell Seas. Emission sources from the South
6856 American continent, identified with back trajectories, were suggested to explain the observed
6857 variations. The yearly mercury evasion from open sea surfaces in the Southern Ocean was estimated to
6858 30 (-450-1700) tons, using the average (and min and max) flux rates obtained in this study. Higher DGM
6859 was measured under sea ice (19-62pgL-1) compared to in open sea due to a capsuling effect, resulting in
6860 a theoretical prevented evasion of 520 (0-3400) tons per year. Diminishing sea ice and higher water
6861 temperatures in polar regions could result in increased mercury evasion to the atmosphere. However,
6862 the contribution of the Southern Ocean to the global modelled annual emissions of mercury from sea
6863 surfaces would probably only be a few percent. (Nerentorp et al 2017).

Hg evasion from contaminated or naturally enrich soils was recognized as important input to regional and global budget (Ferrara et al. 1998, Kotnik et al. 2005). The average evasion flux over urbanized areas and agricultural fields is 5 to 10 times higher than over background soils (Zhu et al. 2016). Measured Hg exchange fluxes over natural enriched surfaces were reported to be 5.5 to 239 (5.6) μg $m^{-2}h^{-1}$, and from anthropogenically contaminated sites 0.001 to 14 (0.6) μg $m^{-2}h^{-1}$ (Zhu et al. 2016 and references therein).

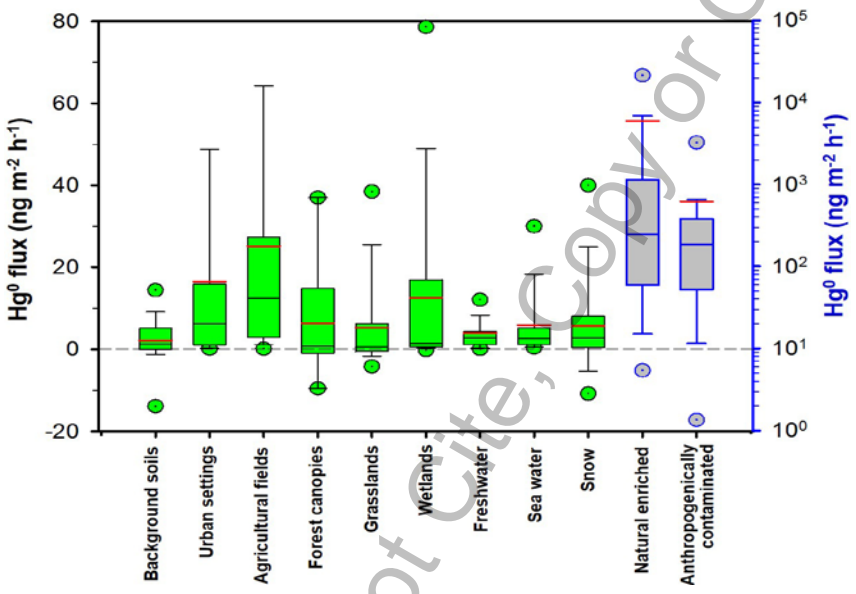

Figure 12: Box and whisker plots of global field-observed GEM fluxes obtained from various landscapes. The two box horizontal border lines indicate 25th and 75th percentiles, whiskers represent 10th and 90th percentiles and outliers (green circles) indicate 5th and 95th percentiles from bottom to top. Red line and black line indicate mean and median flux. Figure from Zhu et al. 2016.

Fluxes from soils, mines and snow surfaces, where GEM can be formed due to photoreduction, are typically higher during daytime as during nighttime (Zhu et al. 2016). Higher evasion flux was observed during warm than cold seasons from different soils and enriched surfaces (Zhu et al. 2016). Hg fluxes measurements over soil, vegetation or snow covered surfaces were consistently higher in E Asia than those measured in Europe, N and S America, Australia and S Africa. This is explained by higher anthropogenic emissions and re-emissions of deposited Hg (Zhu et al. 2016 and references therein).

3.5 Existing data by new monitoring technologies and new methods

Complex commercial instruments as well as sensors and sensing systems have been recently redesigned and improved by introducing innovative technologies. Thus, many sensors have been developed to detect the several forms of mercury making use of nanotechnology. Over the last 20 years, biomolecules, macromolecules, nanostructures (rods, tubes, fibres, particles, dots) and nanocomposite based systems have been found to be the most intriguing and effective detecting devices for mercury detection in several environmental compartments. Most of them have exploited the strong affinity between mercury and gold, others the affinity of mercury ions to specific biomolecules. The possibility to manipulate and investigate the features of the nanomaterials allowed the chance of fabricating selective and more sensitive tools. The Table 11 comprises some of the most recent technologies used to develop sensors and devices for mercury detection.

Table 11: Recent technologies used to develop sensors and devices for mercury detection.

Sampling	Materials/device	Linearity range	LOD	Samples	Reference
Hg ions	CV-AAS +SDS-coated chromosorb P + 2-mercaptobenzoxazole	0.05-85.6 $ngml^{-1}$ 0.09-9.6 $ugml^{-1}$	0.01$ngml^{-1}$	Real samples in liquids	Ghaedi, M. et al., 2006, Anal Lett. 39 1171-1185
TGM-Continuous Emission Monitor	Catalysts to oxidize + polymer composites to absorb + chemicals to remove (CVA-AFS)	0.5-1900 ugm^{-3}	0.05ugm^{-3}	Real samples	TEKRAN331OXi (www.tekran.com)
Optical sensors: Hg^{2+}, FRET bio-sensor (gold nanoparticles-DNA)	Fluorescence quenching		40 nM	Water	Miyake, Y. et al., J. Am. Chem. Soc. 2006, 128, 2172−2173
Optical sensors: Hg^{2+}, surface energy transfer probe-Rhodamine B-AuNPs	Fluorescence quenching		2 ppt	Buffer solution, water, river water, contaminated soil	Darbha, G.K., et al., ACS Nano 2007, 1, 208−214.
Optical sensor: surface-enhanced resonance Raman scattering (SERRS) sensor	structure-switching double stranded DNAs (dsDNAs)		100 pM	Aqueous solution	Kang T., et al. Chemistry. 2011 17(7):2211-4
Electrochemical sensors: Hg^{2+}, array of 256 gold microelectrodes	anodic stripping voltammetry	$5x10^{-8}$-$1x10^{-6}$ M	3.2 µg L^{-1} (16 nM)	Chloride media	Ordeig, O., eta al., Electroanalysis 2006 18 573-578
FET sensors: Hg^{2+}	Thioglycolic acid (TGA)-functionalized -AuNPs-reduced graphene oxide		$2.5x10^{-8}$ M	Aqueous solution	Chen, K., et al., Anal. Chem. 2012, 84, 4057-406

	(rGO)				
Colorimetric sensors: Hg^{2+} (naked eye)	Au-nanorods/glass	2.0 μgl^{-1} to 0.58 mgl^{-1}	$1ugl^{-1}$	Aqueous solution	Chemnasiri W., et al., Sens Actuat B 173 (2012) 322-328
LSPR (prediction model)	Au-nanorods (shift wavelength)		4.5 attograms (mass)	Hg^0 vapour	James J.Z., et al., Analyst 2013
Conductive sensors	CNT-AuNP		2 ppbv	Hg^0 vapour	McNicholas T.P., et al., J. Phys. Chem. C, 2011, 115 13927–13931
Conductive sensors	TiO2NFs-AuNPs (tens of min)		2pptv	Hg^0 vapour	Macagnano A., et al. (a), Sensors and Actuators B 247 (2017) 957–967
Conductive sensors	TiO2NF-AuNPs	20-100 ppbv	1.5 ppbv	Hg^0 vapour	Macagnano et al. (b), ACP 2017 (acp-2016-1077)
QCM sensor (AT cut quartz)	nanostructured gold electrode		2.5 ppbv	Hg^0 vapour	Kabir K.M., et al., Journal of Sensors 2015 ID 727432
Jerome® J405 Mercury Vapour Analyzer	gold thin film (750 ccmin-1)	0.5-999ugm^{-3}	0.5ugm^{-3}	Hg^0 vapour	www.azi.com

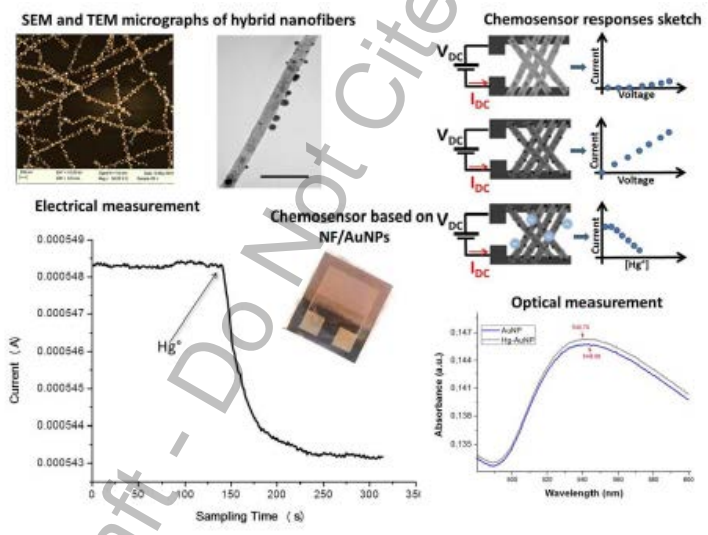

Figure 13: Recent results about sensors based on electrospinning technology: nanofibers of titania doped with AuNPs to detect traces of elemental mercury in air (*Macagnano et al., 2017, a,b).*

However, given the uncertainty and restrictions associated with automated measurements, passive sampling systems currently are a useful alternative for making regional and global estimates of air Hg concentrations. Some passive samplers applied for Hg have been biological materials. Further passive samplers have been designed using a variety of synthetic materials (like sulphur-impregnated carbon (SIC), chlorine-impregnated carbon (CIC), bromine-impregnated carbon (BIC) gold-coated (GCS)

sorbents, etc.) (Li, H. et al., 2017) and housings for Hg collection (McLagan et al., 2016). These latter samplers work on the basis of diffusion. Additionally, surrogate surfaces have been developed for passive measurement of Hg dry deposition. Most commercially available passive/diffusive samplers are planar or axial in shape and offer lower sampling rates and limited sampling capacity. As a result, sensitivity can suffer during short-term analysis (due to low sampling rates), or long-term sampling (analyte back-diffusion due to low capacity). (Huang et al. 2014). Alternatively, radial samplers, consisting of a columnar sorbent surrounded by a cylindrical diffusive barrier, have the purpose to increase the sampling rate by maximizing the surface area across which diffusion occurs (Radiello®, Krol et al., 2010). PASs have been designed with also external shields to protect the sampler components from direct wind, sunlight, and precipitation and to reduce turbulent airflow. A collection of passive samplers more recently developed has been reported in Table 12.

Table 12 – Passive and active samplers developed in recent years to measure TGM [ng m^3] and GOM [pg m^3].

Target	Location	TGM GOM	Materials/sampler	Sampling rate (ml min^{-1})	Blank	DL (pg m^3)	Influences	Reference
TGM	Rural	i) 1-4 ii) 0.8-1.5	i) Gold coated plate ii) silver wire /radial sampler	i) 87 (lab); 51+/-19 (field); 260 theoretical ii) 20 (measured); 33 (theoretical)	i) ii) 80 pg	i) 90 (3 days) ii) 430 (3 days)		Gustin et al., Atmos. Environ., 2011, 45, 5805–5812
TGM	Industrial	25	Gold solution with LDPE/passive integrative mercury sampler (PIMS)	1.4	0.3 ng	2000 (4 weeks)		Brumbaugh et al., Chemosphere: Global Change Sci., 2000, 2, 1–9
TGM	Chamber	10	Gold coated tube/laboratory scale	57 (measured) 114 (theoretical)	0.02 ng	50 (2.8 days); 140 (1 day)	Wind speed	Skov et al., Environ. Chem., 2007, 4, 75–80
TGM	Chamber, indoor, outdoor	2-3.5	Gold-coated silica/axial sampler	0.22 (measured) 0.32 (theoretical)		30% (uncertainty)		Brown et al., J. Environ. Monit., 2012, 14, 2456–2463
TGM	Industrial, suburban, rural	2-5.5	Sulphur-impregnated carbon/axial sampler	90		80 (30 days)	Wind speed	Zhang et al., Atmos. Environ., 2012, 47, 26–32.
TGM	Industrial	2	Gold-coated filter-cation exchange membrane/two-bowl sampler	460 (measured) 556 (theoretical)	0.17 ng	10 (3 days)	Wind speed; humidity	Huang et al., J. Environ. Monit., 2012, 14, 2976–2982
TGM	Chamber, indoor,	1.35−2.16 ng m^{-3}	Sulphur impregnated	0.158-0.121 $m^3 day^{-1}$		11-12 months		Mc. Lagan D., et al.,

	outdoor	(indoor); d 1.17–3.29 ng m^{-3} (outdoor)	carbon sampler/radial in a protective shield	(indoor-outdoor)				Environ. Sci. Technol. Lett. 2016, 3, 24–29
GOM	Rural, suburban	DL-65	Cation-exchange membrane/multiple configurations	0.7-3.2 (measured) 0.055 (theoretical)	0.27 ng to 0.68 ng	5 (2 weeks)	Wind speed	Lyman et al., Atmos. Environ., 2010, 44, 246–252
GOM	Remote	DL-67	Cation-exchange membrane/aerohead configuration		0.56 ng	2.3 (2 weeks)	Wind speed	Wright et al., Science of The Total Environment, 2013, 470–471, 1099–1113
GOM	Industrial, suburban, rural	DL-35	Cation-exchange membrane/ two-bowl sampler	1042 (measured) 486 (theoretical)	0.02-0.04 ng	3 (3 days)	Wind speed; humidity	Huang et al., J. Environ. Monit., 2012, 14, 2976–2982

3.6 Conclusions

To be completed with key highlights on:

- Regional distributions / gradients and time trends
- Gaps in air monitoring spatial coverage
- Limitation of current methods/technology for Hg monitoring in ambient air and fluxes
- The need to foster the development of advanced sensor technology for monitoring mercury concentrations in ambient air, deposition fluxes and gaseous mercury evasions.

In order to come up with a feasible and sustainable strategy for long-term monitoring of Hg in air it is necessary to promote a close cooperation between existing monitoring networks (national, regional, global) with the aims:

- To ensure sustainability of a long-term monitoring program covering both hemispheres
- To assure comparability among different monitoring data sets by promoting the adoption of common SOPs and QA/QC criteria/methods
- To promote intercomparison experiments for testing and validating new methods and technologies for mercury monitoring
- To support Nations in developing their own monitoring programs by promoting a continuous capacity building and transfer of knowledge program in cooperation with UN Environment.

6942 Many experiences already done in past years in the framework of different programs and
6943 projects may be of great help in the future.

6944

3.7 References

Aas, W., Pfaffhuber, K.A., & Nizzetto, P.B. (2016). Heavy metals and POP measurements, 2014 (EMEP/CCC, 04/2016). Kjeller: NILU.

Ambrose, J.L., Gratz, L.E., Jaffe, D.A., Campos, T., Flocke, F., Knapp, D., Stechman, D., Stell, M., Weinheimer, A., Cantrell, C., and Mauldin, R. Mercury Emission Ratios from Coal-Fired Power Plants in the Southeastern United States during NOMADSS. Envir. Sci. Tech. 49 (17), 10389–10397, doi: 10.1021/acs.est.5b01755, 2015.

Amos, H.M., D.J. Jacob, D.G. Streets, E.M. Sunderland. 2013. Legacy impacts of all-time anthropogenic emissions on the global mercury cycle. Global Biogeochemical Cycles. 27, 1-12.

Amos, H.M., D.J. Jacob, D. Kocman, H.M. Horowitz, Y. Zhang, S. Dutkiewicz, M. Horvat, E.S. Corbitt, D.P. Krabbenhoft, E.M. Sunderland. 2014. Global biogeochemical implications of mercury discharges from rivers and sediment burial. Environmental Science and Technology. 48, 9514-9522.

Angot, H., Barret, M., Magand, O., Ramonet, M., and Dommergue, A.: A 2-year record of atmospheric mercury species at a background Southern Hemisphere station on Amsterdam Island, Atmos. Chem. Phys., 14, 11461–11473, doi:10.5194/acp-14-11461-2014, 2014.

Angot, H., Dastoor, A., De Simone, F., Gårdfeldt, K., Gencarelli, C.N., Hedgecock, I.M., Langer, S., Magand, O., Mastromonaco, M.N., Nordstrøm, C., Pfaffhuber, K.A., Pirrone, N., Ryjkov, A., Selin, N.E., Skov, H., Song, S., Sprovieri, F., Steffen, A., Toyota, K., Travnikov, O., Yang, X., Dommergue, A., 2016a. Chemical cycling and deposition of atmospheric mercury in polar regions: review of recent measurements and comparison with models. Atmos Chem Phys 16, 10735–10763. doi:10.5194/acp-16-10735-2016

Angot, H., Dion, I., Vogel, N., Legrand, M., Magand, O., Dommergue, A., 2016b. Multi-year record of atmospheric mercury at Dumont d'Urville, East Antarctic coast: continental outflow and oceanic influences. Atmos Chem Phys 16, 8265–8279. doi:10.5194/acp-16-8265-2016.

Angot, H., Magand, O., Helmig, D., Ricaud, P., Quennehen, B., Gallée, H., Del Guasta, M., Sprovieri, F., Pirrone, N., Savarino, J., Dommergue, A., 2016c. New insights into the atmospheric mercury cycling in central Antarctica and implications on a continental scale. Atmos Chem Phys 16, 8249–8264. doi:10.5194/acp-16-8249-2016.

Ariya, P.A., Dastoor, A.P., Amyot, M., Schroeder, W.H., Barrie, L., Anlauf, K., Raofie, F., Ryzhkov, A., Davignon, D., Lalonde, J., Steffen, A., 2004. The arctic: a sink for mercury. Tellus 56B, 397cling.

Aspmo, K., Temme, C., Berg, T., Ferrari, C., Gauchard, P-A., Fain, X., Wibetoe, G., 2004. Mercury in the atmosphere, snow and melt water ponds in the North Atlantic Ocean during Arctic summer. Environ. Sci. Thecnol 40, 4083–4089.

Banic, C.M., Beauchamp, S.T., Tordon, R.J., Schroeder, W.H., Steffen, A., Anlauf, K.A., Wong, K.H.T. Vertical distribution of gaseous elemental mercury in Canada, J. Geophys. Res. 108, D9, 4264.

Bargagli, R., 2016. Atmospheric chemistry of mercury in Antarctica and the role of cryptogams to assess deposition patterns in coastal ice-free areas. Chemosphere 163, 202–208. doi:10.1016/j.chemosphere.2016.08.007

Bash, J. O. and Miller, D. R.: A note on elevated total gaseous mercury concentrations downwind from an agriculture field during tilling, Sci. Total Environ., 388, 379–388, 2007.

Bash, J. O. and Miller, D. R.: A relaxed eddy accumulation system for measuring surface fluxes of total gaseous mercury, J. Atmos. Ocean. Tech., 25, 244–257, 2008.

Berg, T., Bartnicki, J., Munthe, J., Lattila, H., Hrehoruk, J., Mazur, A., 2001. Atmospheric mercury species in the European Arctic: measurements and modelling. Atmos. Environ. 35, 2569016/j.

Berg, T., Pfaffhuber, K.A., Cole, A.S., Engelsen, O., Steffen, A., 2013. Ten-year trends in atmospheric mercury concentrations, meteorological effects and climate variables at Zeppelin, Ny-Alesund. Atmospheric Chem. Phys. 13, 6575–6586.

Berg, T., Sommar, J., W.A. Cg, Gardfeldt, K., Munthe, J., Schroeder, B., 2003. Arctic mercury depletion events at two elevations as observed at the Zeppelin Station and Dirigibile Italia, Ny-Ålesund, spring 2002. J Phys IV Fr. 107, 151–154.

Brenninkmeijer, C.A.M. P., Crutzen, T., Dauer, D.B., Ebinghaus, R., Filippi, D., Fischer, H., Franke, H., Freiß, U. J., Heintzenberg, H.M., Kock, H.H., Leuenberger, M., Martinsson, B.G., Miemczyk, S., Nguyen, H.N., Oram, D., O'Sullivan, S., Penkett, U., Platt, M., Pupek, M., Ramonet, B., Reichelt, R.M., Rhee, T.S., Rohwer, J., Rosenfeld, K., Scharffe, D., Schlager, H., Schumann, U., Slemr, F., Sprung, D., Stock, P., Thaler, R., van Velthoven, P., Waibel, A., Wandel, A., Waschitschek, K., Wiedensohler, A., Zahn, A., Zech, U., Ziereis H.(2007): Civil Aircraft for the Regular Investigation of the Atmosphere Based on an

Instrumented Container; the new CARIBIC system, Atmospheric Chemistry and Physics, 7, 5277–5339, 2007.

Brooks, S., Saiz-Lopez, A., Skov, H., Lindberg, S.E., Plane, J.M.C., Goodsite, M.E., 2006. The mass balance of mercury in the springtime arctic environment. Geophys. Res. Lett. 33, L13812. doi:10.1029/2005GL025525.

Brooks, S.B., Arimoto, R., Lindberg, S.E., Southworth, G., 2008a. Antarctic polar plateau snow surface conversion of deposited oxidized mercury to gaseous elemental mercury with fractional long-term burial. Atmos. Environ. 42, 2877–2884.

Brooks, S.B., Lindberg, S.E., Southworth, G., Arimoto, R., 2008b. Springtime atmospheric mercury speciation in the McMurdo, Antarctica coastal region. Atmos. Environ. 42, 2885th fra.

Butler, T. J., Cohen, M. D., Vermeylen, F. M., Likens, G. E., Schmeltz, D., & Artz, R. S. (2008). Regional precipitation mercury trends in the eastern USA, 1998–2005: Declines in the Northeast and Midwest, no trend in the Southeast. Atmospheric Environment, 42(7), 1582-1592.

Carbone, F., M. S. Landis, C. N. Gencarelli, A. Naccarato, F. Sprovieri, F. De Simone, I. M. Hedgecock, **N. Pirrone** (2016) Sea surface temperature variation linked to elemental mercury concentrations measured on Mauna Loa. *Geophysical Research Letters*, *43*, doi:10.1002/2016GL069252.

Carpi, A., Fostier, A. H., Orta, O. R., dos Santos, J. C., and Gittings, M.: Gaseous mercury emissions from soil following forest loss and land use changes: Field experiments in the United States and Brazil, Atmos. Environ., 96, 423–429, 2014.

Choi, H. D. and Holsen, T. M.: Gaseous mercury emissions from unsterilized and sterilized soils: The effect of temperature and UV radiation, Environ. Poll., 157, 1673–1678, 2009.

Cole, A.S., Steffen, A., Pfaffhuber, K.A., Berg, T., Pilote, M., Poissant, L., Tordon, R., Hung, H., 2013. Ten-year trends of atmospheric mercury in the high Arctic compared to Canadian sub-Arctic and mid-latitudes sites. Atmospheric Chem. Phys. 13, 1535–1545.

Cole, A. S., Steffen, A., Eckley, C. S., Narayan, J., Pilote, M., Tordon, R., Graydon, J. A., St Louis, V. L., Xu, X., & Branfireun, B. (2014). A Survey of Mercury in Air and Precipitation across Canada: Patterns and Trends. Atmosphere, 5, 635-668.

Colette, A., Aas, W., Banin, L., Braban, C.F., Ferm, M., González Ortiz, A., Ilyin, I., Mar, K., Pandolfi, M., Putaud, J.-P., Shatalov, V., Solberg, S., Spindler, G., Tarasova, O., Vana, M., Adani, M., Almodovar, P., Berton, E., Bessagnet, B., Bohlin-Nizzetto, P., Boruvkova, J., Breivik, K., Briganti, G., Cappelletti, A., Cuvelier, K., Derwent, R., D'Isidoro, M., Fagerli, H., Funk, C., Garcia Vivanco, M., González Ortiz, A., Haeuber, R., Hueglin, C., Jenkins, S., Kerr, J., de Leeuw, F., Lynch, J., Manders, A., Mircea, M., Pay, M.T., Pritula, D., Putaud, J.-P., Querol, X., Raffort,V., Reiss, I., Roustan, Y., Sauvage, S., Scavo, K., Simpson, D., Smith, R.I., Tang, Y.S., Theobald, M., Tørseth, K., Tsyro, S., van Pul, A., Vidic, S., Wallasch, M., Wind, P. (2016). Air pollution trends in the EMEP region between 1990 and 2012. Joint Report of the EMEP Task Force on Measurements and Modelling (TFMM), Chemical Co-ordinating Centre (CCC), Meteorological Synthesizing Centre-East (MSC-E), Meteorological Synthesizing Centre-West (MSC-W) (EMEP: TFMM/CCC/MSC-E/MSC-W Trend Report) (EMEP/CCC, 01/2016). Kjeller: NILU.

Converse, A. D., Riscassi, A. L., and Scanlon, T. M.: Seasonal variability in gaseous mercury fluxes measured in a high-elevation meadow, Atmos. Environ., 44, 2176–2185, 2010. doi:10.1029JD002116, 2003.

D'Amore F., M. Bencardino, S. Cinnirella, F. Sprovieri, **N. Pirrone** (2015) Data quality through a web-based QA/QC system: implementation for atmospheric mercury data from the Global Mercury Observation System. *Environmental Science: Processes Impacts*, 2015, DOI:10.1039/C5EM00205B.

Dastoor, A., Ryzhkov, A., Durnford, D., Lehnherr, I., Steffen, A., Morrison, H., 2015. Atmospheric mercury in the Canadian Arctic. Part II: Insight from modeling. Sci. Total Environ., Special Issue: Mercury in Canada's North 509–510, 16–27. doi:10.1016/j.scitotenv.2014.10.112

Dommergue, A., Barret, M., Courteaud, J., Cristofanelli, P., Ferrari, C.P., Gall 2015. Atmospheric mercury in the Canadian Arctic. Part II: Insight frondary layer of the Antarctic Plateau. Atmos Chem Phys 12, 11027–11036. doi:10.5194/acp-12-11027-2012

Dommergue, A., Larose, C., Faurteaud, J., Cristofanelli, P., Ferrari, C.P., Gall 2015. Atmospheric mercury in the Canadian Arctic. Part II: Insight frondar-Ålesund Area (79°N) and Their Transfer during Snowmelt. Environ. Sci. Technol. 44, 901–907. doi:10.1021/es902579m.

Dommergue, A., Ferrari, C. P., Gauchard, P.-A., Boutron, C. F., Poissant, L., Pilote, M., Jitaru, P., and Adams, F. C.: The fate of mercury species in a sub-arctic snowpack during snowmelt, Geophys. Res. Lett., 30, 1621, doi:10.1029/2003GL017308, 2003.

7054 Ebinghaus, R., Jennings, S., Kock, H., Derwent, R., Manning, A., and Spain, T.: Decreasing trends in total gaseous
7055 mercury observations in baseline air at Mace Head, Ireland from 1996 to 2009, Atmos. Environ., 45, 3475–
7056 3480, 2011.
7057 Ebinghaus, R., Kock, H. H., Coggins, A. M., Spain, T. G., Jennings, S. G., and Temme, C.: Long-term
7058 measurements of atmospheric mercury at Mace Head, Irish west coast, between 1995 and 2001, Atmos.
7059 Environ., 36, 5267–5276, 2002.
7060 Ebinghaus, R., Kock, H.H., Temme, C., Einax, J.W., Lowe, A.G., Richter, A., Burrows, J.P., Schroeder, W.H.,
7061 2002. Antarctic springtime depletion of atmospheric mercury. Environ. Sci. Technol. 36, 123876, 20.
7062 Ebinghaus, R., Slemr, F. Aircraft measurements of atmospheric mercury over southern and eastern Germany,
7063 Atmos. Environ. 34, 895-903, 2000.
7064 Ebinghaus, R., Slemr, F., Brenninkmeijer, C.A.M., van Velthoven, P., Zahn, A., Hermann, M., O´Sullivan,
7065 D.A.,Oram, D.E. Emissions of gaseous mercury from biomass burning in South America in 2005 observed
7066 during CARIBIC flights, Geophys. Res. Lett. 34, L08813, doi:10.1029/2006GL028866, 2007.
7067 Ericksen, J. A., Gustin, M. S., Schorran, D. E., Johnson, D. W., Lindberg, S. E., and Coleman, J. S.: Accumulation
7068 of atmospheric mercury in forest foliage, Atmos. Environ., 37, 1613–1622, 2003.
7069 Faïn, X., Grangeon, S., Bahlmann, E., Fritsche, J., Obrist, D., Dommergue, A., Ferrari, C. P., Cairns, W., Ebinghaus,
7070 R., and Barbante, C.: Diurnal production of gaseous mercury in the alpine snowpack before snowmelt, J.
7071 Geophys. Res.-Atmos., 112, D21311, doi:10.1029/2007JD008520, 2007.
7072 Ferrara, R., Maserti, B. E., Andersson, M., Edner, H., Ragnarson, P., Svanberg, S., and Hernandez, A.: Atmospheric
7073 mercury concentrations and fluxes in the Almadén district (Spain), Atmos. Environ., 32, 3897–3904, 1998.
7074 Ferrari, C.P., Gauchard, P.-A., Aspmo, K., Dommergue, A., Magand, O., Bahlmann, E., Nagorski, S., Temme, C.,
7075 Ebinghaus, R., Steffen, A., Banic, C., Berg, T., Planchon, F., Barbante, C., Cescon, P., Boutron, C.F., 2005.
7076 Snow-to-air exchanges of mercury in an arctic seasonal snowpack in Ny-Alesund, Svalbard. Atmos.
7077 Environ. 39, 7633–7645.
7078 Fisher, J.A., D.J. Jacob, A.L. Soerensen, H.M. Amos, A. Steffen, E.M. Sunderland. 2012. Riverine source of Arctic
7079 Ocean mercury inferred from atmospheric observations. Nature Geoscience. 5: 499-504.
7080 Friedli, H.R., Radke, L.F., Lu, J.Y., Banic, C.M., Leaitch, W.R., MacPherson, J.I. Mercury emissions from burning
7081 of biomass from temperate North American forests: laboratory and airborne measurements, Atmos.
7082 Environ, 37, 253-267, 2003.
7083 Fritsche, J., Obrist, D., Zeeman, M. J., Conen, F., Eugster, W., and Alewell, C.: Elemental mercury fluxes over a
7084 sub-alpine grassland determined with two micrometeorological methods, Atmos. Environ., 42, 2922–2933,
7085 2008.
7086 Fu, X., Feng, X., Zhang, H., Yu, B., and Chen, L.: Mercury emissions from natural surfaces highly impacted by
7087 human activities in Guangzhou province, South China, Atmos. Environ., 54, 185– 193, 2012a.
7088 Fu, X.W., Zhang, H., Yu, B.,Wang, X., Lin, C.-J., and Feng, X. B.: Observations of atmospheric mercury in China:
7089 a critical review, Atmos. Chem. Phys., 15, 9455–9476, doi:10.5194/acp-15-9455- 2015, 2015.
7090 Gratz, L., et al. Airborne Observations of Mercury Emissions from the Chicago/Gary Urban/Industrial Area during
7091 the 2013 NOMADSS Campaign. Atmos. Env., 145, 415–423, doi: 10.1016/j.atmosenv.2016.09.051, 2016.
7092 Gratz, L.E., et al. Oxidation of mercury by bromine in the subtropical Pacific free troposphere. Geophys. Research
7093 Letters, 42, 10492–10502, doi: 10.1002/2015GL066645, 2015.
7094 Graydon, J.A., V. St. Louis, S. Lindberg, K.A. Sandilands, J.W.M. Rudd, C.A. Kelly, R. Harris, M. Tate, D.P.
7095 Krabbenhoft, C.A. Emmerton, H. Asmath, M. Richardson. The role of terrestrial vegetation in atmospheric
7096 Hg deposition: Pools and fluxes from the METAALICUS experiment. Global Biogeochemical Cycles,
7097 2012, 2610.1029/2011GB004031.
7098 Grigal, D. F.: Mercury sequestration in forests and peatlands: A review, J. Environ. Qual., 32, 393–405, 2003.
7099 Gustin, M. and Jaffe, D.: Reducing the Uncertainty in Measurement and Understanding of Mercury in the
7100 Atmosphere, Environ. Sci. Technol., 44, 2222–2227, 2010.
7101 Gustin, M. S., Biester, H., and Kim, C. S.: Investigation of the light-enhanced emission of mercury from naturally
7102 enriched substrates, Atmos. Environ., 36, 3241–3254, 2002.
7103 Gustin, M. S., Ericksen, J. A., Schorran, D. E., Johnson, D. W., Lindberg, S. E., and Coleman, J. S.: Application of
7104 controlled mesocosms for understanding mercury air-soil-plant exchange, Environ. Sci. Technol., 38,
7105 6044–6050, 2004.
7106 Gustin, M. S.: Exchange of mercury between the atmosphere and terrestrial ecosystems, in: Environmental
7107 Chemistry and Toxicology of Mercury, edited by: Liu, G. L., Cai, Y., and O'Driscoll, N., 423–451, 2011.
7108 Gustin, M.; Jaffe, D. Reducing the uncertainty in measurement and understanding of mercury in the atmosphere.
7109 Environ. Sci. Technol. 2010, 44, 2222–2227.

Gustin, M.S.; Lindberg, S.E.; Weisberg, P.J. An update on the natural sources and sinks of atmospheric mercury. Appl. Geochem. 2008, 23, 482–493.

Han, Y., Huh, Y., Hong, S., Hur, S.D., Motoyama, H., 2014. Evidence of air-snow mercury exchange recorded in the snowpack at Dome Fuji, Antarctica. Geosci. J. 18, 105i, 3. doi:10.1007/s12303-013-0054-7.

Han, Y., Huh, Y., Hong, S., Hur, S.D., Motoyama, H., Fujita, S., Nakazawa, F., Fukui, K., 2011. Quantification of total mercury in Antarctic surface snow using ICP-SF-MS: spatial variation from the coast to Dome Fuji. Bull. Korean Chem. Soc. 32, 4258–4264.

Han, Y., Huh, Y., Hur, S.D., Hong, S., Chung, J.W., Motoyama, H., 2017. Net deposition of mercury to the Antarctic Plateau enhanced by sea salt. Sci. Total Environ. 583, 81patial variation from thtenv.2017.01.008.

Hararuk, O., D. Obrist, Y. Luo. 2013. Modeling the sensitivity of soil mercury to climate-induced changes in soil-carbon pools. Biogeosciences. 10, 2393-2407.

Hartman, J. S., Weisberg, P. J., Pillai, R., Ericksen, J. A., Kuiken, T., Lindberg, S. E., Zhang, H., Rytuba, J. J., and Gustin, M. S.: Application of a rule-based model to estimate mercury exchange for three background biomes in the Continental United States, Environ. Sci. Technol., 43, 4989–4994, 2009.

Hirdman, D., Aspmo, K., Burkhart, J.F., Eckhardt, S., Sodemann, H., Stohl, A., 2009. Transport of mercury in the Arctic atmosphere: Evidence for a spring-time net sink and summer-time source. Geophys. Res. Lett. 36, L12814. doi:10.1029/2009GL038345.

Horowitz, HM, DJ Jacob, Y Zhang, TS Dibble, HM Amos, JA Schmidt, ES Corbitt, EA Marais, EM Sunderland. (2017). A new mechanism for atmospheric mercury redox chemistry: implications for the global mercury budget. Atmospheric Chemistry and Physics. 17, 6353-6371.

Kalinchuk, V.V., Mishukov, V.F., Astakhov, A.S., 2017. Arctic source for elevated atmospheric mercury (Hg0) in the western Bering Sea in the summer of 2013. J. Environ. Sci. doi:10.1016/j.jes.2016.12.022

Kim, S. H., Han, Y. J., Holsen, T. M., & Yi, S. M. (2009). Characteristics of atmospheric speciated mercury concentrations (TGM, Hg (II) and Hg (p)) in Seoul, Korea. Atmospheric Environment, 43(20), 3267-3274.

Kirk, J. L., St. Louis, V. L., and Sharp, M. J.: Rapid reduction and reemission of mercury deposited into snowpacks during atmospheric mercury depletion events at Churchill, Manitoba, Canada, Environ. Sci. Technol., 40, 7590–7596, 2006.

Kock, H., Bieber, E., Ebinghaus, R., Spain, T., and Thees, B.: Comparison of long-term trends and seasonal variations of atmospheric mercury concentrations at the two European coastal monitoring stations Mace Head, Ireland, and Zingst, Germany, Atmos. Environ., 39, 7549–7556, 2005.

Kocman, D. and Horvat, M.: A laboratory based experimental study of mercury emission from contaminated soils in the River Idrijca catchment, Atmos. Chem. Phys., 10, 1417–1426, doi:10.5194/acp-10-1417-2010, 2010.

Kotnik, J., Horvat, M., and Dizdarevic, T.: Current and past mercury distribution in air over the Idrija Hg mine region, Slovenia, Atmos. Environ., 39, 7570–7579, 2005.

Król, S., Zabiegała, B., and Namiesnik, J.: Monitoring VOCs in atmospheric air II. Sample collection and preparation, TRACTrend. Anal. Chem., 29, 1101–1112, 2010.

Kwon, S.Y., Selin, N.E., 2016. Uncertainties in Atmospheric Mercury Modeling for Policy Evaluation. Curr. Pollut. Rep. 2, 103–114. doi:10.1007/s40726-016-0030-8.

Lalonde, J. D., Poulain, A. J., and Amyot, M.: The role of mercury redox reactions in snow on snow-to-air mercury transfer, Environ. Sci. Technol., 36, 174–178, 2002.

Larose, C., Dommergue, A., De Angelis, M., Cossa, D., Averty, B., Marusczak, N., Soumis, N., Schneider, D., Ferrari, C., 2010. Springtime changes in snow chemistry lead to new insights into mercury methylation in the Arctic. Geochim. Cosmochim. Acta 74, 6263–6275.

Lehnherr, I., & St. Louis, V. (2009). Importance of ultraviolet radiation in the photodemethylation of methylmercury in freshwater ecosystems. Environmental Science and Technology, 43(15), 5692-5698.

Lin, C. J., Gustin, M. S., Singhasuk, P., Eckley, C., and Miller, M.: Empirical models for estimating mercury flux from soils, Environ. Sci. Technol., 44, 8522–8528, 2010.

Lin, H., Zhang, W., Deng, C. et al. Evaluation of passive sampling of gaseous mercury using different sorbing materials, Environ Sci Pollut Res (2017) 24: 14190. doi:10.1007/s11356-017-9018-1

Lindberg, S. E., Zhang, H., Gustin, M., Vette, A., Marsik, F., Owens, J., Casimir, A., Ebinghaus, R., Edwards, G., Fitzgerald, C., Kemp, J., Kock, H. H., London, J., Majewski, M., Poissant, L., Pilote, M., Rasmussen, P., Schaedlich, F., Schneeberger, D., Sommar, J., Turner, R.,Wallschlager, D., and Xiao, Z.: Increases in mercury emissions from desert soils in response to rainfall and irrigation, J. Geophys. Res.-Atmos., 104, 21879–21888, 1999.

Lindberg, S.; Bullock, R.; Ebinghaus, R.; Engstrom, D.; Feng, X.B.; Fitzgerald, W.; Pirrone, N.; Prestbo, E.;Seigneur, C. A synthesis of progress and uncertainties in attributing the sources of mercury in deposition. Ambio 2007, 36, 19–32.

Lindberg, S.E., Brooks, S., Lin, C.-J., Scott, K., Meyers, T., Chambers, L., Landis, M., Stevens, R., 2001. Formation of Reactive Gaseous Mercury in the Arctic: Evidence of Oxidation of Hg. Res.-Atd irrigation, J. Geophys. Resrctic Sunrise. Water Air Soil Pollut. Focus 1, 295–302. doi:10.1023/a:1013171509022

Lindberg, S.E., Brooks, S., Lin, C.-J., Scott, K.J., Landis, M.S., Stevens, R.K., Goodsite, M.E., Richter, A., 2002. Dynamic oxidation of gaseous mercury in the arctic troposphere at polar sunrise. Environ. Sci. Technol. 36, 1245ic Sun.

Lu, J.Y., Schroeder, W.H., 2004. Annual time-series of total filterable atmospheric mercury concentrations in the Arctic. Tellus 56B, 213–222.

Lu, J.Y., Schroeder, W.H., Barrie, L.A., Steffen, A., Welch, H.E., Martin, K., Lockhart, L., Hunt, R.V., Boila, G., Richter, A., 2001. Magnification of atmospheric mercury deposition to polar regions in springtime: the link to tropospheric ozone depletion chemistry. Geophys. Res. Lett. 28, 3219–3222.

Lyman, S.N., Jaffe, D.A. Formation and fate of oxidized mercury in the upper troposphere and lower stratosphere, Nature Geoscience, doi:10.1038/NGEO1353, 2011.

Macagnano A., Perri V., Zampetti E., Bearzotti A., De Cesare F., Sprovieri F., Pirrone N. A smart nanofibrous material for adsorbing and detecting elemental mercury in air. Atmos. Chem. Phys., 17, 6883-6893, 2017. Https://doi.org/10.5194/acp-17-6883-2017 (b)

Macagnano A., Perri V., Zampetti E., Ferretti A.M., Sprovieri F., Pirrone N., Bearzotti A., Esposito G., De Cesare F. Elemental mercury vapor chemoresistors employing TIO_2 nanofibers photocatalytically decorated with Au-nanoparticles. Sensors and Actuators B 247 (2017) 957–967 (a)

Mann, E. A., Mallory, M. L., Ziegler, S. E., Avery, T. S., Tordon, R., and O'Driscoll, N. J.: Photoreducible mercury loss from Arctic snow is influenced by temperature and snow age, Environ. Sci. Technol., 49, 12120–12126, 2015.

Maxwell, J. A., Holsen, T. M., and Mondal, S.: Gaseous elemental mercury (GEM) emissions from snow surfaces in Northern New York, PloS One, 8, e69342, 2013.

Mazur, M., Mitchell, C. P. J., Eckley, C. S., Eggert, S. L., Kolka, R. K., Sebestyen, S. D., and Swain, E. B.: Gaseous mercury fluxes from forest soils in response to forest harvesting intensity: A field manipulation experiment, Sci. Total Environ., 496, 678–687, 2014.

McLagan D.S., Mazur M.E.E., Mitchell C.P.J., Wania F. Passive air sampling of gaseous elemental mercury: a critical review. Atmos. Chem. Phys., 16, 3061-3076, 2016. Http://www.atmos-chem-phys.net/16/3061/2016/; doi:10.5194/acp-16-3061-2016.

Moore, C. W., Obrist, D., Steffen, A., Staebler, R. M., Douglas, T. A., Richter, A., & Nghiem, S. V. (2014). Sea Ice Lead-induced Convective Forcing of Mercury and Ozone in the Arctic Boundary Layer. Nature

Nerentorp Mastromonaco, M., G, Eckley, C. S., Eggert, S. L., Kolka, R. K., Sebfors, A., Ahnoff, M., Dommergue, A., Meld manipulation experiment, Sci. Total Environ., 496, 678harvesting intensity: A field manipulation experimentn. 129, 125l Env.

Nerentorp Mastromonaco, M., Gårdfeldt, K., Langer, S., Dommergue A., Seasonal Study of Mercury Species in the Antarctic Sea Ice Environment. Environ. Sci. Technol. 50 (23), pp 12705–12712, 2016b.

Nerentorp Mastromonaco, M., Gårdfeldt, K., , Assmann, K M., Langerc, S., Delalid, T., Shlyapnikovd, M Y., Zivkovicd, I., Horvat, M. Speciation of mercury in the waters of the Weddell, Amundsen and Ross Seas (Southern Ocean) Marine Chemistry Volume 193, 20 July 2017, Pages 20–33, 2017.

Nerentorp Mastromonaco, M., Gårdfeldt, K., Jourdain, B., Abrahamsson, K., Granfors, A., Anhoff, M., Dommergue, A., Mejan, G., Jacobi, H-W. 2016 a Antarctic winter mercury and ozone depletion events over sea ice. Atmospheric Environment, 129:125-132, 2016a.

Nerentorp Mastromonaco, M., Gårdfeldt, K., Langer, S. Seasonal Flux of mercury over west Antarctic Seas. Marine Chemistry 193 20:44-54, 2017.

Nghiem, S., Rigor, I., Richter, A., Burrows, J. P., Shepson, P. B., Bottenheim, J., Barber, D. G., Steffen, A., Latonas, J., Wang, F., Stern, G., Clemente-Colón, P., Martin, S., Hall, D. K., Kaleschke, L., Tackett, P., Neumann, G., & Asplin, M. J. (2012). Field and satellite observations of the formation and distribution of Arctic atmospheric bromine above a rejuvenated sea ice cover. Journal of Geophysical Research D: Atmospheres, 117(5), D00S05.

Nguyen, H. T., Kim, K. H., Kim, M. Y., Hong, S., Youn, Y. H., Shon, Z. H., & Lee, J. S. (2007). Monitoring of atmospheric mercury at a global atmospheric watch (GAW) site on An-Myun Island, Korea. Water, air, and soil pollution, 185(1-4), 149-164.

Nguyen, H. T., Kim, M. Y., & Kim, K. H. (2010). The influence of long-range transport on atmospheric mercury on Jeju Island, Korea. Science of the Total Environment, 408(6), 1295-1307.

Osawa, T., Ueno, T., & Fu, F. (2007). Sequential variation of atmospheric mercury in Tokai‐mura, seaside area of eastern central Japan. Journal of Geophysical Research: Atmospheres, 112(D19).

Pacyna, E. G., Pacyna, J. M., Fudala, J., Strzelecka-Jastrzab, E., Hlawiczka, S., and Panasiuk, D.: Mercury emissions to the atmosphere from anthropogenic sources in Europe in 2000 and their scenarios until 2020, Sci. Total Environ., 370, 147–156, 2006.

Pfaffhuber, K.A., Berg, T., Hirdman, D., Stohl, A., 2012. Atmospheric mercury observations from Antarctica: seasonal variation and source and sink region calculations. Atmos Chem Phys 12, 3241–3251. doi:10.5194/acp-12-3241-2012.

Pierce, A.H.; Moore, C.W.; Wohlfahrt, G.; HÖrtang, L.; Kljun, N.; Obrist, D. Eddy covariance flux measurements of gaseous elemental mercury using cavity ring-down spectroscopy. Environ. Sci. Technol. 2015, 49, 1559–1568.

Pirrone, N., Hedgecock, I., and Sprovieri, F.: Atmospheric mercury, easy to spot and hard to pin down: impasse?, Atmos. Environ., 42, 8549–8551, doi:10.1016/j.atmosenv.2008.09.004, 2008.

Poissant, L., Pilote, M., 2003. Time series analysis of atmospheric mercury in Kuujjuarapik/Whapmagoostui (Quebec). J Phys IV Fr. 107, 10798551,

Poissant, L.; Pilote, M.; Beauvais, C.; Constant, P.; Zhang, H.H. A year of continuous measurements of three atmospheric mercury species (GEM, RGM and Hgp) in southern Quebec, Canada. Atmos. Environ. 2005, 39, 1275–1287.

Poulain, A. J., Lalonde, J. D., Amyot, J. D., Shead, J. A., Raofie, F., & Ariya, P. A. (2004). Redox transformations of mercury in an Arctic snowpack at springtime. Atmospheric Environment, 38, 6763-6774.

Prestbo, E. M., & Gay, D. A. (2009). Wet deposition of mercury in the US and Canada, 1996–2005: Results and analysis of the NADP mercury deposition network (MDN). Atmospheric Environment, 43(27), 4223-4233.

ResSteffen, A., Douglas, T., Amyot, M., Ariya, P., Aspmo, K., Berg, T., Bottenheim, J., Brooks, S., Cobbett, F., Dastoor, A., Dommergue, A., Ebinghaus, R., Ferrari, C., Gardfeldt, K., Goodsite, M.E., Lean, D., Poulain, A.J., Scherz, C., Skov, H., Sommar, J., Temme, C., 2008. A synthesis of atmospheric mercury depletion event chemistry in the atmosphere and snow. Atmos Chem Phys 8, 1445–1482. doi:10.5194/acp-8-1445-2008.

Risch, M. R., Gay, D. A., Fowler, K. K., Keeler, G. J., Backus, S. M., Blanchard, P., ... & Dvonch, J. T. (2012). Spatial patterns and temporal trends in mercury concentrations, precipitation depths, and mercury wet deposition in the North American Great Lakes region, 2002–2008. Environmental pollution, 161, 261-271.

Schartup, AT, U. Ndu, P.H. Balcom, R.P. Mason, E.M. Sunderland. 2015. Contrasting effects of marine and terrestrially derived organic matter on mercury speciation and bioavailability in seawater. Environmental Science and Technology. 49: 5965-5972.

Schroeder, W. H., Beauchamp, S., Edwards, G., Poissant, L., Rasmussen, P., Tordon, R., Dias, G., Kemp, J., Van Heyst, B., and Banic, C. M.: Gaseous mercury emissions from natural sources in Canadian landscapes, J. Geophys. Res.-Atmos., 110, D18302, 2005.

Schroeder, W.H., Anlauf, K.G., Barrie, L.A., Lu, J.Y., Steffen, A., Schneeberger, D.R., Berg, T., 1998. Arctic spingtime depletion of mercury. Nature 394, 331 sout.

Selin, N. E., Jacob, D. J., Yantosca, R. M., Strode, S., Jaeglé, L., and Sunderland, E. M.: Global 3-D land-ocean-atmosphere model for mercury: Present-day versus preindustrial cycles and anthropogenic enrichment factors for deposition, Global Biogeochem. Cy., 22, GB2011, doi:10.1029/2007GB003040, 2008.

Shah, V., Jaeglé, L., Gratz, L.E., Ambrose, J.L., Jaffe, D.A., Selin, N.E., Song, S., Giang A., et al. Origin of oxidized mercury in the summertime free troposphere over the Southeast United States. Atmos. Chem. Phys., 16, 1511–1530, doi: 10.5194/acp-16-1511-2016, 2016.

Shanley, J. B., Engle, M. A., Scholl, M., Krabbenhoft, D. P., Brunette, R., Olson, M. L., & Conroy, M. E. (2015). High mercury wet deposition at a “clean air” site in Puerto Rico. Environmental Science & Technology, 49(20), 12474-12482.

Sheu, G. R., Lin, N. H., Wang, J. L., Lee, C. T., Yang, C. F. O., & Wang, S. H. (2010). Temporal distribution and potential sources of atmospheric mercury measured at a high-elevation background station in Taiwan. Atmos. Environ. 2010, *44*(20), 2393-2400.

Sillman, S., Marsik, F., Dvonch, J. T., & Keeler, G. J. (2013, January). Assessing atmospheric deposition of mercury in Florida, USA: Local versus global sources and models versus measurements. In E3S Web of Conferences (Vol. 1). EDP Sciences.

Skov, H. Brooks, S. Goodsite, M.E. Lindberg, S.E. Meyers, T.P. Landis, M.S. Larsen, M.R.B. Jensen, B. McConville, G. Christensen, J. (2006) Measuring reactive gaseous mercury flux by relaxed eddy accumulation. Atm. Env. vol 40, 5452-5463.

Skov, H. Christensen, J. Goodsite, M.E. Heidam, N.Z. Jensen, B. Wåhlin, P. and Geernaert, G. (2004) "The fate of elemental mercury in Arctic during atmospheric mercury depletion episodes and the load of atmospheric mercury to Arctic" ES & T. vol. 38, 2373-2382. . doi:10.1021/es030080h.

Skov, H. Sørensen, B.T. Landis, M.E. Johnson, M.S. Lohse, C. Goodsite, M.E. and Sacco, P. (2007) Performance of a new diffusive sampler for Hgo determination in the troposphere. Environmental Chemistry, vol. 4. 75-80.

Skov, H., Christensen, J.H., Goodsite, M.E., Heidam, N.Z., Jensen, B., With reduced sulfur groups, Environ. Sci. T. Sci. Tr groups, Environ. Sci. Tci. Ton with reduced sulfur groups, Environ. Sci. Tn. Sci. Tn.hnol., 40, 4174si180, 2006.iences.viron. Sci. Technol. 38, 2373–2382. doi:10.1021/es030080h

Skyllberg, U., Bloom, P. R., Qian, J., Lin, C. M., and Bleam, W. F.: Complexation of mercury(II) in soil organic matter: EXAFS evidence for linear two-coordination with reduced sulfur groups, Environ. Sci. Technol., 40, 4174–4180, 2006.

Slemr, F., Angot, H., Dommergue, A., Magand, O., Barret, M., Weigelt, A., Ebinghaus, R., Brunke, E.-G., Pfaffhuber, K. A., Edwards, G., Howard, D., Powell, J., Keywood, M., and Wang, F.: Comparison of mercury concentrations measured at several sites in the Southern Hemisphere, Atmos. Chem. Phys., 15, 3125–3133, doi:10.5194/acp-15-3125-2015, 2015.

Slemr, F., Brunke, E.-G., Ebinghaus, R., and Kuss, J.: Worldwide trend of atmospheric mercury since 1995, Atmos. Chem. Phys., 11, 4779–4787, doi:10.5194/acp-11-4779-2011, 2011.

Slemr, F., Ebinghaus, R., Brenninkmeijer, C.A.M., Hermann, M., Kock, H.H., Martinsson, B.G., Schuck, T.,Sprung, D., van Velthoven, P., Zahn, A., Ziereis, H. Gaseous mercury distribution in the upper troposphere and lower stratosphere observed onboard the CARIBIC passenger aircraft, Atmos. Chem. Phys. 9, 1957-1969, 2009.

Slemr, F., Ebinghaus, R., Brenninkmeijer, C.A.M., Hermann, M., Kock, H.H., Levine, I., Martinsson, B., Schuck, T., Sprung, D., van Velthoven, P., Zahn, A., Ziereis H.: Gaseous mercury distribution in the upper troposphere and lower stratosphere observed during the CARIBIC flights from Frankfurt to southern China and to South America, Atmospheric Chemistry and Physics, 9 (6): 1957-1969, 2009.

Slemr, F., Ebinghaus, R., Weigelt, A., Kock, H. H., Brenninkmeijer, C. A. M., Schuck, T., Hermann, M., et al.: CARIBIC observations of gaseous mercury in the upper troposphere and lower stratosphere. E3S Web of Conferences, 1(2013), 17001. (doi:10.1051/e3sconf/20130117001), 2013.

Slemr, F.; Brenninkmeijer, C.A.; Rauthe-Schöch, A.; Weigelt, A.; Ebinghaus, R.; Brunke, E.-G.; Martin, L.; Spain, T.G.; O´Doherty, S.: El Niño–Southern Oscillation influence on tropospheric mercury concentrations. Geophysical Research Letters 43, 1766–1771 (doi:10.1002/2016GL067949), 2016a.

Slemr, F.; Weigelt, A.; Ebinghaus, R.; Brenninkmeijer, C.; Baker, A.; Schuck, T.; Rauthe-Schöch, A.; Riede, H., Leedham, E.; Hermann, M.; van Velthoven, P.; Oram, D.; O'Sullivan, D.; Dyroff, C.; Zahn, A.; Ziereis, H.: Mercury Plumes in the Global Upper Troposphere Observed during Flights with the CARIBIC Observatory from May 2005 until June 2013, Atmosphere, 5, 342-369; doi:10.3390/atmos5020342, 2014.

Slemr, F.; Weigelt, A.; Ebinghaus, R.; Kock, H.H.; Bödewadt, J.; Brenninkmeijer, C.A.M.; Rauthe-Schöch, A.; Weber, S.; Hermann, M.; Becker, J.; Zahn, A.; Martinsson, B.: Atmospheric mercury measurements onboard the CARIBIC passenger aircraft. Atmospheric Measurement Techniques 9, 2291–2302 (doi: 10.5194/amt-9-2291-2016), 2016b.

Smith-Downey, N.V., E.M. Sunderland, D.J. Jacob. 2010. Anthropogenic impacts on global storage and emissions of mercury from terrestrial soils: Insights from a new global model. Journal of Geophysical Research, 115, G03008.

Soerensen, A., Skov, H., Soerensen, D. J. B., and Johnson, M.: Global concentrations of gaseous elemental mercury and reactive gaseous mercury in the marine boundary layer, Environ. Sci. Technol., 44, 7425–7430, doi:10.1021/es903839n, 2010a.

Soerensen, A., Sunderland, E., Holmes, C., Jacob, D., Yantosca, R., Skov, H., Christensen, J., Strode, S., and Mason, R.: An improved global model for air-sea exchange of mercury: high concentrations over the North Atlantic, Environ. Sci. Technol., 44, 8574–8580, doi:10.1021/es102032g, 2010b.

Soerensen, A.L., D.J. Jacob, A.T. Schartup, J.A. Fisher, I. Lehnherr, V.L. St. Louis, L-E. Heimberger, J.E. Sonke, D.P. Krabbenhoft, E.M. Sunderland. (2016). A mass budget for mercury and methylmercury in the Arctic Ocean. Global Biogeochemical Cycles, 30, 560–575, doi:10.1002/2015GB005280.

Soerensen, A.L., D.J. Jacob, D.G. Streets, M.L.I. Witt, R. Ebinghaus, R.P. Mason, M. Andersson, E.M. Sunderland. 2012. Multi-decadal decline of mercury in the North Atlantic atmosphere explained by changing subsurface seawater concentrations. Geophysical Research Letters, 39, L21810.

Soerensen, A.L., R.P. Mason, P.H. Balcom, D.J. Jacob, Y. Zhang, J. Kuss, E.M. Sunderland. 2014. Elemental mercury concentrations and fluxes in the tropical atmosphere and ocean. Environmental Science and Technology. 48, 11312-11319.

Soerensen, A.L., R.P. Mason, P.H. Balcom, E.M. Sunderland. 2013. Drivers of surface ocean mercury concentrations and air-sea exchange in the West Atlantic Ocean. Environmental Science and Technology. 47, 7757-7765.

Sommar, J., Andersson, M. E., and Jacobi, H.-W.: Circumpolar measurements of speciated mercury, ozone and carbon monoxide in the boundary layer of the Arctic Ocean, Atmos. Chem. Phys., 10, 5031–5045, doi:10.5194/acp-10-5031-2010, 2010.

Sommar, J., W, Sunderland, E., Holmes, C., Jacob, D., Yantosca, R., Skov, H., Christensen, J., Strode, S., and Mason, R.: ACircumpolar transport and air-surface exchange of atmospheric mercury at Ny- over the North ASvalbard, spring 2002. Atmos Chem Phys 7, 151–166. doi:10.5194/acp-7-151-2007.

Sprovieri F., N. Pirrone, M.S. Landis, R.K. Stevens (2005a) Oxidation of gaseous elemental mercury to gaseous divalent mercury during 2003 polar sunrise at Ny-Alesund. Environmental Science & Technology 39 (23), 9156-9165.

Sprovieri F., N. Pirrone, M.S. Landis, R.K. Stevens (2005b) Atmospheric mercury behavior at different altutudes at Ny Alesund during Spring 2003. Atmospheric Environment 39 (39), 7646-7656.

Sprovieri, F., Pirrone, N., Bencardino, M., D'Amore, F., Angot, H., Barbante, C., Brunke, E.-G., Arcega-Cabrera, F., Cairns, W., Comero, S., Diéguez, M. D. C., Dommergue, A., Ebinghaus, R., Feng, X. B., Fu, X., Garcia, P. E., Gawlik, B. M., Hageström, U., Hansson, K., Horvat, M., Kotnik, J., Labuschagne, C., Magand, O., Martin, L., Mashyanov, N., Mkololo, T., Munthe, J., Obolkin, V., Ramirez Islas, M., Sena, F., Somerset, V., Spandow, P., Vardè, M., Walters, C., Wängberg, I., Weigelt, A., Yang, X., and Zhang, H.: Five-year records of mercury wet deposition flux at GMOS sites in the Northern and Southern hemispheres, Atmos. Chem. Phys., 17, 2689-2708, doi:10.5194/acp-17-2689-2017, 2017.Temme, C., Blanchard, P., Steffen, A., Banic, C., Beauchamp, S., Poissant, L., Tordon, R., andWiens, B.: Trend, seasonal and multivariate analysis study of total gaseous mercury data from the Canadian atmospheric mercury measurement network (CAMNet), Atmos. Environ., 41, 5423–5441, 2007.

Sprovieri, F., Pirrone, N., Bencardino, M., D'Amore, F., Angot, H., Barbante, C., Brunke, E.-G., Arcega-Cabrera, F., Cairns, W., Comero, S., Diéguez, M. D. C., Dommergue, A., Ebinghaus, R., Feng, X. B., Fu, X., Garcia, P. E., Gawlik, B. M., Hageström, U., Hansson, K., Horvat, M., Kotnik, J., Labuschagne, C., Magand, O., Martin, L., Mashyanov, N., Mkololo, T., Munthe, J., Obolkin, V., Ramirez Islas, M., Sena, F., Somerset, V., Spandow, P., Vardè, M., Walters, C., Wängberg, I., Weigelt, A., Yang, X., and Zhang, H.: Five-year records of mercury wet deposition flux at GMOS sites in the Northern and Southern hemispheres, Atmos. Chem. Phys., 17, 2689-2708, doi:10.5194/acp-17-2689-2017, 2017.Stamenkovic, J., Gustin, M. S., Arnone, J. A., Johnson, D. W., Larsen, J. D., and Verburg, P. S. J.: Atmospheric mercury exchange with a tallgrass prairie ecosystem housed in mesocosms, Sci. Total Environ., 406, 227–238, 2008.

Sprovieri, F., Pirrone, N., Ebinghaus, R., Kock, H., and Dommergue, A.: A review of worldwide atmospheric mercury measurements, Atmos. Chem. Phys., 10, 8245–8265, doi:10.5194/acp-10-8245-8265, 2010, 2010.

Sprovieri, F., Pirrone, N., Hedgecock, I.M., Landis, M.S., Stevens, R.K., 2002. Intensive atmospheric mercury measurements at Terra Nova Bay in antarctica during November and December 2000. J. Geophys. Res. 107, 4722. doi:10.1029/2002JD002057

Steffen, A., Bottenheim, J., Cole, A., Douglas, T. A., Ebinghaus, R., Friess, U., Netcheva, S., Nghiem, S., Sihler, H., & Staebler, R. (2013). Atmospheric mercury over sea ice during the OASIS-2009 campaign. Atmospheric Chemistry and Physics, 13, 7007-7021.

Steffen, A., Bottenheim, J., Cole, A., Ebinghaus, R., Lawson, G., Leaitch, W.R., 2014. Atmospheric mercury speciation and mercury in snow over time at Alert, Canada. Atmospheric Chem. Phys. 14, 2219-2231.

Steffen, A., Schroeder, W., Macdonald, R., Poissant, L., Konoplev, A., 2005. Mercury in the Arctic atmosphere: An analysis of eight years of measurements of GEM at Alert (Canada) and a comparison with observations at Amderma (Russia) and Kuujjuarapik (Canada). Sci. Total Environ., Sources, Occurrence, Trends and Pathways of Contaminants in the ArcticBidleman S.I. 342, 185–198. doi:10.1016/j.scitotenv.2004.12.04.

Sunderland, EM, RP Mason. (2007) Human impacts on open ocean mercury concentrations. Global Biogeochemical Cycles. GB4022, doi:10.1029/2006GB002876, 2007.

Swartzendruber, P. C., Jaffe, D.A., Finley, B., 2009. Development and First Results of an Aircraft-Based, High Time Resolution Technique for Gaseous Elemental and Reactive (Oxidized) Gaseous Mercury. Environ. Sci. Technol. 43, 7484–7489.

Temme, C., Einax, J.W., Ebinghaus, R., Schroeder, W.H., 2003. Measurements of atmospheric mercury species at a coastal site in the antarctic and over the atlantic ocean during polar summer. Environ. Sci. Technol. 37, 22ol.

Tørseth, K., Aas, W., Breivik, K., Fjæraa, A.M., Fiebig, M., Hjellbrekke, A.G., Lund Myhre, C., Solberg, S., Yttri, K.E. (2012). Introduction to the European Monitoring and Evaluation Programme (EMEP) and observed atmospheric composition change during 1972-2009. Atmospheric Chemistry and Physics, 12, 5447-5481. doi:10.5194/acp-12-5447-2012.

UNEP, 2015. Global mercury modelling: update of modelling results in the global mercury assessment 2013.

UNEP, GLOBAL REVIEW OF MERCURY MONITORING NETWORKS, 1- 48, November 2016.

Wang, J., Zhang, L., Xie, Z., 2016. Total gaseous mercury along a transect from coastal to central Antarctic: Spatial and diurnal variations. J. Hazard. Mater. 317, 362 Guizhou,:10.1016/j.jhazmat.2016.05.068

Wang, S. F., Feng, X. B., Qiu, G. L., Fu, X. W., and Wei, Z. Q.: Characteristics of mercury exchange flux between soil and air in the heavily air-polluted area, eastern Guizhou, China, Atmos. Environ., 41, 5584–5594, 2007.

Weigelt, A., Ebinghaus, R., Manning, A., Derwent, R., Simmonds, P., Spain, T., Jennings, S., and Slemr, F.: Analysis and interpretation of 18 years of mercury observations since 1996 at Mace Head, Ireland, Atmos. Environ., 100, 85–93, doi:10.1016/j.atmosenv.2014.10.050, 2015.

Weigelt, A., Ebinghaus, R., Pirrone, N., Bieser, J., Bödewadt, J., Esposito, G., Slemr, F., van Velthoven, P. F. J., Zahn, A., and Ziereis, H.: Tropospheric mercury vertical profiles between 500 and 10 000m in central Europe, Atmos. Chem. Phys., 16, 4135–4146, doi:10.5194/acp-16-4135-2016, 2016.

Weigelt A., Franz Slemr, Ralf Ebinghaus, Nicola Pirrone, Johannes Bieser, Jan Bödewadt, Giulio Esposito, and Peter F. J. van Velthoven (2016) Mercury emissions of a coal-fired power plant in Germany**.** *Atmospheric Chemistry & Phys*ics, 16, 13653-13668, doi:10.5194/acp-16-13653-2016, 2016.

Weigelt, A.; Temme, C.; Bieber, E.; Schwerin, A.; Schuetze, M.; Ebinghaus, R.; Kock, H.H. : Measurements of atmospheric mercury species at a German rural background site from 2009 to 2011 – methods and results, Environmental Chemistry, 10(2), 102-110 (DOI: 10.1071/EN12107), 2013.

Weiss-Penzias, P. S., Gay, D. A., Brigham, M. E., Parsons, M. T., Gustin, M. S., & ter Schure, A. (2016). Trends in mercury wet deposition and mercury air concentrations across the US and Canada. Science of the Total Environment, 568, 546-556.

Xin, M. and Gustin, M. S.: Gaseous elemental mercury exchangewith low mercury containing soils: Investigation of controlling factors, Appl. Geochem., 22, 1451–1466, 2007.

Yang, Y. K., Zhang, C., Shi, X. J., Lin, T., andWang, D. Y.: Effect of organic matter and pH on mercury release from soils, J. Environ. Sci., 19, 1349–1354, 2007.

Yu, J., Xie, Z., Kang, H., Li, Z., Sun, C., Bian, L., Zhang, P., 2014. High variability of atmospheric mercury in the summertime boundary layer through the central Arctic Ocean. Sci. Rep. 4, 6091. doi:10.1038/srep06091.

Zhang, Y., D.J. Jacob, H.M. Horowitz, L. Chen, H.M. Amos, D.P. Krabbenhoft, F. Slemr, V.L. St. Louis, E.M. Sunderland. Observed dcrease in atmospheric mercury explained by global decline in anthropogenic emissions. Proceedings of the United States National Academy of Sciences. 113(3): 526-531.

Zhang, Y., D.J. Jacob, S. Dutkiewicz, H.M. Amos, M.S. Long, E.M. Sunderland. (2015). Biogeochemical drivers of the fate of riverine mercury discharged to the global and Arctic oceans. Global Biogeochemical Cycles, 29, 854-864.

Zhu W., Lin CJ., Wang X., Sommar J., Fu X., and Feng X., Global observations and modeling of atmosphere–surface exchange of elemental mercury: a critical review. Atmos. Chem. Phys., 16, 4451–4480, 2016.